EVALUATING THE IMPACTS OF LAND USE LAND COVER CHANGE ON STREAMFLOW AND SEDIMENT YIELD: A CASE STUDY OF MODJO WATERSHED, AWASH RIVER BASIN, ETHIOPIA

MULUKEN LAMBIYE LAGISSO

A THESIS SUBMITTED TO

THE DEPARTMENT OF WATER RESOURCES ENGINEERING

SCHOOL OF CIVIL ENGINEERING AND ARCHITECTURE

PRESENTED IN PARTIAL FULFILLMENT OF THE REQUIREMENT FOR THE DEGREE OF MASTER'S IN WATER RESOURCES ENGINEERING (SPECIALIZATION IN IRRIGATION ENGINEERING)

OFFICE OF GRADUATE STUDIES

ADAMA SCIENCE AND TECHNOLOGY UNIVERSITY

JUNE, 2021
ADAMA, ETHIOPIA

EVALUATING THE IMPACTS OF LAND USE LAND COVER CHANGE ON STREAMFLOW AND SEDIMENT YIELD: A CASE STUDY OF MODJO WATERSHED, AWASH RIVER BASIN, ETHIOPIA

MULUKEN LAMBIYE LAGISSO

ID NO. PGE/18846/11

ADVISOR

DR. BOJA MEKONNEN

A THESIS SUBMITTED TO

THE DEPARTMENT OF WATER RESOURCES ENGINEERING

SCHOOL OF CIVIL ENGINEERING AND ARCHITECTURE

PRESENTED IN PARTIAL FULFILLMENT OF THE REQUIREMENT FOR THE DEGREE OF MASTER'S IN WATER RESOURCES ENGINEERING (SPECIALIZATION IN IRRIGATION ENGINEERING)

OFFICE OF GRADUATE STUDIES

ADAMA SCIENCE AND TECHNOLOGY UNIVERSITY

JUNE, 2021

ADAMA, ETHIOPIA

DECLARATION

I hereby declare that this Master Thesis entitled ***''Evaluating the Impacts of Land Use Land Cover Change on Streamflow and Sediment Yield: A Case Study of Modjo Watershed, Awash River Basin, Ethiopia"*** is my original work. That is, it has not been submitted for the award of any academic degree, diploma or certificate in any other university. All sources of materials that are used for this thesis have been duly acknowledged through citation.

Muluken Lambiye Lagisso	_____	_____
Name of the student	Signature	Date

RECOMMENDATION

I, the advisor of this thesis, hereby certify that I have read the revised version of the thesis entitled ***''Evaluating the Impacts of Land Use Land Cover Change on Streamflow and Sediment Yield: A Case Study of Modjo Watershed, Awash River Basin, Ethiopia"*** prepared under my guidance by Muluken Lambiye Lagisso submitted in partial fulfillment of the requirements for the degree of Mater's of Science in Water Resources Engineering (Specialization in Irrigation Engineering).

Therefore, I recommend the submission of revised version of the thesis to the Department following the applicable procedures.

Dr. Boja Mekonnen _____ _____

Major Advisor Signature Date

APPROVAL PAGE OF M.Sc. THESIS

I, the advisor of the thesis entitled ***''Evaluating the Impacts of Land Use Land Cover Change on Streamflow and Sediment Yield: A Case Study of Modjo Watershed, Awash River Basin, Ethiopia"*** and Developed by Muluken Lambiye Lagisso, hereby certify that the recommendation and suggestions made by the board of examiners are appropriately incorporated into the final version of the thesis.

Dr. Boja Mekonnen _____ _____

Major Advisor Signature Date

We, the undersigned, members of the Board of Examiners of the thesis by Muluken Lambiye Lagisso have read and evaluated the thesis entitled ***''Evaluating the Impacts of Land Use Land Cover Change on Streamflow and Sediment Yield: A Case Study of Modjo Watershed, Awash River Basin, Ethiopia"*** and examined the candidate during open defense. This is, therefore, to certify that the thesis is accepted for partial fulfillment of the requirement of the degree of Master of Science in Water Resources Engineering (Specialization in Irrigation Engineering).

_____ _____ _____

Chairperson Signature Date

_____ _____ _____

Internal Examiner Signature Date

_____ _____ _____

External Examiner Signature Date

Final approval and acceptance of the thesis is contingent upon submission of its final copy

To the Office of Postgraduate Studies (OPGS) through the Department Graduate Council

(DGC) and School Graduate Committee (SGC).

Department Head	Signature	Date
School Dean	Signature	Date
Office of Postgraduate Studies,	Dean Signature	Date

ACKNOWLEDGMENT

First and above all, I would like to praise the Lord who is Alpha and Omega for giving me this great success in academic journey. Next, I wish to express my deepest gratitude to those who helped me during Academic journey.

I would like to pay my special regards to my Major Advisor Dr. Boja Mekonnen for his most Invaluable support and Encouragement during my Thesis work. I really appreciate his commitment, dedication and so quick responses during my thesis work. I also would like to pay my special regards to Water Resources Engineering Department.

I wish to show my gratitude to all Doctors who gave me courses, department head and for those who showed me ways and directions professionally. I would like thank National Meteorology agency; Ministry of water, Irrigation and Energy for providing necessary data to my research work.

I would like express my deepest gratitude to my beloved wife Elsabeth Tesfaye, and my beloved twin daughters Elzira Muluken and Eliana Muluken. You handled all those difficulties and challenges in my absence for the classes. My special gratitude is extended to my parents Mr. Lambiye Lagisso and Mrs. Tireza Kidanemariyam for their financial support and encouragement since childhood; my brothers and my sisters also thankful. I also would like to thank Mr. Tesfaye Genjebo and Mrs. Workinesh Bashawu for caring my family in Hossana during my absence for the class.

Finally, I wish to show my gratitude to Mr. Sisiay Bekele and Mrs. Aster Ismael. I wish to thank Mr. Mitiku Teshome, Mr. Alexander Takele, Mr. Samuel Kassa, Mr. Kiya Kefeni Mr. Yossef Dentamo and all the people whose assistance was a milestone in the completion of this project.

TABLE OF CONTENTS

LIST OF TABLES

LIST OF FIGURES

LIST OF TABLES IN THE APPENDIX

LIST OF FIGURES IN THE APPENDIX

LIST OF ABBREVIATIONS

ERDAS	Earth Resources Data Analysis System
ETM	Enhanced Thematic Mapper Plus
FAO	Food Agricultural Organization
GIS	Geography Information System
HEC-HMS	Hydrologic Engineering Center -Hydrologic Modeling System
HRU	Hydrologic Response Unit
HBV	Hydrologiska Byrans Vattenavdelning
IHDP	International Human Dimension Program
IDW	Inverse Distance Weighting
LULCC	Land Use Land Cover Change
MLC	Maximum Likelihood Classifier
MoWR	Ministry of Water Resource
MUSLE	Modified Universal Soil Losses Equation
NMSA	National Metrological Service Agency
TM	Thematic Mapper
SWRRB	Simulator for Water Resources in Rural Basin model
SWAT	Soil and Water Assessment Tool
SWAT-CUP	SWAT Calibration and Uncertainty Procedures
USDA-ARS	US Department of Agriculture – Agriculture Research Service

ABSTRACT

Water resources study under watershed level requires hydrological models in order to design, plan and manage the water resources. The main objective of this study is to evaluate the impacts of land use land cover change on stream flow and sediment yield. Modjo watershed is experiencing significant land use land cover dynamics due to urbanization effects and population growth. SWAT model is a semi distributed physically based hydrological model, and GIS and remote sensing application tool is used under this study. The model was calibrated and validated at Modjo gauging station. Highly increasing amount of stream flow and sediment yield has been directly drains to Koka dam which is a major problem the watershed facing. Input parameters are hydrological data (stream flow and sediment yield), meteorological data (temperature, precipitation, relative humidity, and wind speed and sunshine hour), DEM, soil map, and land use land cover map were generated using GIS. Land use land cover classification was done by ERDAS IMAGINE 2014 application for four (1989, 1999, 2009 and 2018) periods. Land use land cover classes of the watershed are agricultural land, shrub land, forest, bare land, built-up and water body. Supervised classification technique using maximum likelihood classifier was applied during classification. The overall accuracy results of the classified images were 87.22 %, 90.56%, 91.67% and 89.44%, and kappa coefficient values were 0.82, 0.87, 0.89 and 0.84, respectively for the years 1989, 1999, 2009 and 2018. The performance of the model was evaluated using statistical indices. The statistical analysis of calibration results for Modjo watershed showed satisfactory agreement between observed and simulated monthly values. The model calibration and validation indicates R^2=0.76, NSE=0.57, PBIAS= -21.3, for streamflow calibration; R^2=0.78, NSE=0.69, PBIAS=16.6, for streamflow validation. Similarly, R^2=0.71, NSE=0.71, PBIAS=8.0, for sediment yield calibration. R^2=0.86, NSE=0.78, PBIAS= -20.2, for sediment yield validation. Among the 29 sub-catchments, five (sub-catchments 8,7, 9, 25, and 10) produced the highest sediment yield and are more exposed to erosion. The average annual streamflow of Modjo watershed is 416.13mm for 1989 and 487.87mm for 2018, respectively. The mean annual sediment yield of the watershed was 13.93 t/ha/yr and 39.93 t/ha/yr in 1989 and 2018, respectively. In general, the model was capable of simulating streamflow and sediment yield from Modjo watershed.

***Key word**: SWAT Model, Modjo, watershed, Land use land cover change*

CHAPTER ONE

INTRODUCTION

1.1. Background

Land use land cover change has a great influence on the hydrological response of a watershed (Kashaigili and Majaliwa, 2013; Kirby et al., 2016). The hydrological processes which are affected by such changes include evapotranspiration, infiltration, surface runoff, groundwater flow and stream discharge regime (Natkhin et al., 2015). The effects of the land use land cover and climate change on hydrological processes are set to increase in the future due to the increased clearance of virgin forest lands for agriculture and the rise of global warming (Fischer, 2013).

Rapid socio-economic development causes land use land cove changes that include changes of land cover classes, for example, conversion of agriculture or forest to industrialization and residential area due to population growth, in addition alteration within classes such as a change of crop rotations or crops (Wagner et al., 2013). The indicators of land use land cover manifest as the current global environmental concerns such as increasing concentrations of greenhouses gases in the atmosphere, loss of biodiversity and conversion and fragmentation of natural vegetation area (Ellis, 2007).

Land use land cover changes directly affect the condition of water resources mainly through vegetation interception, evapotranspiration, runoff, surface infiltration, soil moisture status, and so forth, thereby affecting the process of watershed hydrology and water resource cycles (Yao et al., 2014). In addition with the above problems land use and cover changes could lead to a decreased availability of different products and services for human, livestock, agricultural production and damage to the environment as well (Agarwal et al., 2002).

Efficient design, planning, and management of river basin projects that deals with conservation and utilization of water for various purposes requires characterization and understanding of stream flow and sediment yield magnitude of a catchment. To accurately determine the quantity of surface runoff and sediment yield that takes place in a river basin, understanding of the complex relationships between rainfall and runoff

processes, which depend upon many geomorphological and climate factor is necessary (Dereje, 2010).

Sediment yield is dependent on gross soil loss in the watershed and on the transport of eroded material out of the watershed. The total amount of sediment that is delivered to the outlet of the watershed is known as the sediment yield (Julien, 2010). It is a result of erosion and deposition processes within a catchment. Sediment yield and transport has been noted for altering the hydrological regimes of river basins (Ayivor and Gordon, 2012).

Watershed models are very important tools for the planning and management of watersheds or river basins. Watershed models can integrate information over a large scale and a long period to simulate various watershed processes such as runoff, soil erosion, and transport of nutrients and pesticides. Deforestation, in appropriate land use practice, soil erosion and land degradation have reached serious proportions, with negative implications on local ecosystem functions and services such as hydrological regimes and soil fertility loss.

The SWAT model was used to simulate the streamflow and sediment yield of Modjo watershed. It is a semi-distributed physical-based hydrological model that has been commonly used for investigating the impacts of land use land cover change on water resources around the world (Garg, 2017). The study basically focuses on evaluating the impacts of land use land cover dynamics on streamflow and sediment yield of Modjo watershed by using semi-distributed physically based hydrological model SWAT and GIS and Remote sensing application.

1.2. Statement of the problem

Despite being considered as a water tower of Africa, Ethiopia is facing significant problems related to water resources, such as flooding, drought and depletion of ecosystem services (Tessema, 2015). The land in the country is less intensive; more land is needed to grow crops with increase population of the country. As a result, deforestation is inevitable and conversion of forest in to agricultural land thereby changing the land use of the

country. Land use land cover changes generate many environmental problems such as biodiversity loss and release of greenhouse gases.

Major problems on the watershed are highly increased amount of streamflow and very high amount of sediment yield in wetter seasons due to considerable expansion in areas under farmland, rapid increase of human and livestock population which is greater than the carrying capacity of the natural resources, expansion of intensive agricultural practice and overgrazing on the area, deforestation due to population increase, intensive wood extraction, urbanization and infrastructure expansion, and presence of rugged terrain. During this time runoff that moves directly to the Modjo river results a reduction of infiltration rates, base-flow and groundwater recharge; and scarcity of water resource availability due to partly declining natural vegetation covers.

Demographic factors like population growth and density, need for additional lands for farming and grazing as well as demands for tree products are drivers and implications of Land use land cover change on Modjo watershed. Increase of soil fertility loss, land degradation, bare land expansion, surface runoff production, soil erosion, and expansion of flood affected areas and sedimentation problems are also another implications of Land use land cover change. The land use land cover plays a fundamental role in driving hydrological processes within a sub basin. These include changes in water demands such as irrigation, changes in water supply from altered hydrological processes of infiltration, groundwater recharge and surface runoff.

Sedimentation and siltation problems in downstream part of the watershed is also a serious challenge which minimizes the total storage capacity of Koka reservoir. Additionally, soil erosion and high surface runoff which leads to occurrence of significant soil nutrient loss in the upstream part. Modjo River which directly drains to Koka reservoir transports sediment to reservoir of Koka dam which directly resulted in life span reduction and unwanted cost for sediment removal.

1.3. Objectives

1.3.1. General Objective

The general objective of the study was to evaluate impacts of Land use land cover dynamics on hydrologic process of stream flow and sediment yield on Modjo watershed of Upper Awash River Basin using physically based semi-distributed hydrological model SWAT (Soil Water Assessment Tool) and GIS and remote sensing application tool.

1.3.2. Specific Objectives

The specific objectives of the study are:

- To assess spatiotemporal variability of Land use land cover change on Modjo watershed for the last 30 years (1989-2018).
- To evaluate the performance of SWAT in simulating historical streamflow and sediment yield in the for Modjo river watershed.
- To analysis land use land cover change on stream flow and sediment yield.

1.4. Research Questions

1. How spatiotemporal variability of Land use land cover change look like in the study area?
2. How streamflow and sediment yield are responding under changing Land use land cover in the study area?
3. How well SWAT model perform in simulating historical streamflow and sediment yield in the Modjo river watershed?

1.5. Significance of the study

Appropriate prediction of streamflow and sediment yield at watershed level helps to manage watershed hydrology of a particular area. Estimation of stream flow and sediment yield by using hydrological models predicts the impact of land use land cover influence practices on water resources, sediment and agricultural yields. Land use land cover change indirectly affects the amount of evapotranspiration, groundwater infiltration and overland runoff. Modjo watershed had experienced extreme flooding, drought, and very high amount of sediment yield. This study quantitatively evaluates adverse impacts of human

activities on the watershed and it helps governmental and non-governmental organizations at both regional as well as national level in putting proper management plans, decisions and mitigation measures to minimize the related problems on the area.

1.6. Scope of the study

Modjo watershed is located in the Upper Awash River Basin Ethiopia. Evaluating the impacts of land use land cover change on stream flow and Sediment yield of the watershed was studied using SWAT model. Land use land cover classification of satellite images were classified by using ERDAS Imagine Software. Model performance evaluation, calibration and validation, analyzing sensitive parameters by using Automatic calibration and uncertainty analysis incorporated in SWAT2012via the SWAT-CUP (SWAT Calibration and Uncertainty Procedures) was used for this study. Land use land cover map was identified using different separate periods of 1989-1999, 2000-2009 and 2009-2018 to show land use land cover change of Modjo watershed.

1.7. Thesis Organization

This thesis was organized into five (5) main parts. The first part (Introduction) contains the background of the study and provides the brief overview of the study undertaken. It also provide the information on why this research done (study problem) as well as its objectives and highlight the significance and scope/limitation of the study. The second part (Literature Review) was emphasized on brief explanation of Land use land cover change on streamflow and sediment yield, Effects of Land use land cover change on surface hydrology, ERDAS Imagine and image classification, Hydrological models, GIS and Remote sensing application. It also contains some of theoretical and empirical work/studies in Ethiopia related to Land use land cover change on streamflow and sediment yield. The third part (Materials and Methods) was explain brief description of the study area, materials used, data required and its source as well as methods of data preparation and analysis used to accomplish the whole objective of the study was described. The fourth part provide the result and discussion of the study corresponding to the research objectives and previous work respectively, and finally (under fifth part) conclusions and recommendations was forwarded at the end of thesis body.

CHAPTER TWO

LITERATURE REVIEW

2.1. Land use land cover change on streamflow and sediment yield

2.1.1. Land use land cover change definition and concepts

Land use and land cover dynamics are widespread, accelerating, and significant processes driven by human actions but also producing changes that impact humans. These dynamics alter the availability of different biophysical resources including soil, vegetation, water, animal feed and others. Consequently, land use and cover changes could lead to a decreased availability of different products and services for human, livestock, agricultural production and damage to the environment as well (Agarwal et al., 2002).

Land use and land cover changes often result from the alteration of natural vegetation for different purposes including logging, urbanization and agriculture. Both globally and at local scales, land use land cover changes generate many environmental problems such as biodiversity loss and release of greenhouse gases (Mukete et al., 2018).

The purposes for which land cover is exploited by humans are varies in time and space in biophysical environments, socioeconomic activities, and cultural contexts is referred to as land-use. From a wider perspective, land cover is often the attributes of the earth's land surface and immediate subsurface including soil, water, topography, and human structures. Here, land cover is known to exist in two forms conversions and modifications where conversions involve a shift from one land cover type to another. On the other hand, land cover modifications involve changes that affect land cover characteristics without changing its overall classification (Lambin, 2003)

Land use land cover change is the shift in intent and/or management constitutes land use and land cover. Land use land cover change can be classified into land use and land cover conversions, and land use and land cover modification. Conversion refers to change from one cover or use type to another, as is the case in agricultural expansion, deforestation, or change in urban extent. Land use and land cover modification, on the other hand, involves

the maintenance of broad cover or use type in the face of change in its attributes. Both conversion and modifications of land use and land cover have important environmental consequences through their impacts on soil and water, biodiversity, and microclimate, hence, contribute to watershed degradation (Stolbovoi, 2002).

2.1.2. Land use land cover change on streamflow

Land use and land cover changes altering hydrological processes and have the potential to exert a large influence on earth water (Kaushal et al., 2017). Rapid socio-economic development causes Land use and land cover changes that include changes of land cover classes, for example, conversion of agriculture or forest to industrialization and residential area due to population growth, in addition alteration with in classes such as a change of crop rotations or crops (Wagner et al., 2013).

Land use and land cover changes has been recognized as a key driver of hydrological processes such as surface runoff, ET and base flow (Zhao et al., 2013 and Garg et al., 2017). Juang et al. (2007) reported that the changes in Land use and land cover have significant effects on atmospheric elements like precipitation and temperature, key driving elements of the hydrological cycle. Thus, it changes the water balance of a watershed that comprises streamflow, base flow and evapotranspiration (Shooshtari et al., 2017). Therefore, examining the practices and consequences of changing Land use and land cover are vital for the hydrologists, ecologists and land managers (Stonestorm et al., 2009; Mallinis et al. 2014).

2.1.3. Land use land cover change on sediment yield

Land use land cover change is an important process of altering the fluxes of water, sediment, contaminants and energy. Mainly caused by human, impact of land use on water resources availability is high. Degraded watersheds tend to accelerate overland flow reducing soil moisture and base flow recharge, and increase sediment detachment and transport. Various studies used land cover mapping tools and method to understand land use changes, inventory of forest and natural resources as well as understand the changes in the hydrologic behavior of watersheds (Mango et al., 2011).

Investigating impacts of land use change on spatio-temporal change of sediment yield can assist water authorities to identify the most vulnerable erosion-prone areas of a catchment. Therefore quantifying the effects of land use change on spatio-temporal change patterns of sediment yield is crucial to development of soil–water resources and land use management at a catchment scale (Tripathi et al., 2005).

The impacts of land use change on sediment yield have received increasingly widespread concern used SWAT model in the Yellow River basin and explored forest will decrease sediment yield and with the increase of land use of agriculture the sediment yield will increase correspondingly. Studied the relationships between soil erosion and sediment yield with vegetation NDVI in the Yellow River indicated that the vegetation status has a significant impact on sediment formation and transport (Toxopeus et al., 2010).
(Mueller et al., 2009) studied the effects of land use change on sediment yield for a meso-scale catchment in the Southern Pyrenees and found that land use change have larger impacts on sediment yield than climate change.

Soil erosion is a natural and dynamic process that occurs when the force of wind, raindrops or runoff on the soil surface exceeds the cohesive agent that binds the soil together. Soil erosion caused by water is a serious problem in many parts of the world which causes most of the degradation of agricultural lands (Ifabiyi, 2004).

Soil erosion accelerated by human activity and has a serious ecological impact that costs a nation due to on-site effects such as soil nutrient and economic loss and offsite effects due to reservoir sedimentation and downstream irrigation and water resources project damages (Upadhya and Pandey, 2012).

2.1.4. Land use and land cover change in Ethiopia

Ethiopia is one of the developing countries where agriculture is the backbone of the economy, and where agriculture is facing a major environmental challenge from land use land cover change (Minta et al., 2017). Studies so far conducted in different parts of Ethiopia reveals different results of land use land cover change impact with different approaches. For instance, (Getahun and Van Lanen, 2015) studied the impact of land use land cover changes of Melka Kuntrie sub basin. The result shows that a slightly higher

stream flows for the land cover changes. Similarly stream flow of Gilgel Abbay watershed has increased, whereas the ground water flow has decreased.

Another study by Jemberie et al. (2016) in Gilgel Abbay catchment indicate that an increase of cultivation, decrease of grass and shrub land caused loosening and movement of a soil layer. Therefore, it caused an increase in sediment yield especially during peak flow periods. (Rientjes et al., 2011) also evaluated the land cover change impact in the Upper Gilgel Abbay catchment of the Upper Blue Nile basin. There is a significant decrease in forest cover mainly due to expansion of agricultural land. As a result the annual and the peak flows of the catchment increased by 13% and 46%, respectively while the low flows decreased by 35%.

Recent studies in the Beressa Watershed Northern Central highland of Ethiopia indicated that forest cover and water body increased due to the involvement of local communities to plant trees around their homestead and farm lands (Tesfa and Gebremariam, 2016). An outspread of agricultural land and settlement and reduction of forest and grass land in Lake Ziway Catchment increased the mean wet monthly flow by 3.8% and decreased dry season flow by 12.3% (Tufa, 2015).

Another study carried out by Setegn et al. (2009) in Alemaya lake Eastern highlands of Ethiopia show that, the area adjacent to the lake are constantly cultivated which aggravated the process of soil erosion and increased the sedimentation of the lake. As a result the volume of water has been decreasing over time. (Welde and Gebremariam, 2017) conducted a similar study in Tekeze dam catchment. The study described that expansion of bare and agricultural land increased mean annual stream flow by 6.02% and sediment yield amounts by 17.39%.

Kassa (2009) assessed watershed hydrological responses to changes in land use land cover and management practices at Hare watershed rift valley basin. The result of the analysis indicated that expansion of crop land contributed to an increase in run-off and reduction on dry-season flows. Similarly farmlands and settlements expansion in Hare watershed mostly associated with the decrease in forest class. As a result, at present the river only satisfies 15.75% of downstream irrigation demand even with 100% diversion during the dry season.

Land use land cover dynamics is very crucial process that needs great investigation and this problem in Ethiopia as developing country have been studied in several parts with different scholars and researchers. Most of these studies indicated that croplands have expanded at the expanse of natural vegetation including forests and shrub lands (Belay, 2002).

According to Kassa (2009), in his study in southern Wello, reported the decline of natural forests and grazing lands due to conversions to croplands (Bewket, 2003) have reported an increase in wood lots (eucalyptus tree plantations) and cultivated land at the expense of grazing land in both Chemoga watershed in north-western Ethiopia, and Sebat-bet Gurage land in south-central Ethiopian. Land use and land cover Changes that occurred from 1971/72 to 2000 in Yerer Mountain and its surrounding results an expansion of cultivated land at the expense of the grasslands (Gebrehiwet, 2004).

According to Hadgu and Kiros (2008) identified that decrease of natural vegetation and expansion of agricultural land over a period of 41 years in Tigray, northern part of Ethiopia. He concluded that population pressure was an important deriver for expansion and intensification of agricultural land in recent periods.

Another study carried out by Garedew (2010) in the semiarid areas of the central Rift Valley of Ethiopia, during the period 1973-2000 cropland coverage has increased and woodland cover lost. Similarly, (Feoli et al., 2002) also reported the expansion of evergreen vegetation with increase of population. Study on a Hare watershed, in Rift Valley of Ethiopia, (Kassa, 2009) reported that due to the replacement of natural forest in to farmland and settlements, the mean monthly discharge for wet months had increased while in the dry season decreased.

In many highlands parts of Ethiopia, agriculture had been gradually expanded from gently sloping land into the steeper slopes of the neighboring mountains. According to many literatures, population that has been steadily increased at a growth rate of 2 to 3% per year during the past five decades is the major cause of this expansion. Projected estimates show that the population of the country will be double in 40 years' time (UN Population Division, 2008). In some areas, expansions of cultivation, commonly into steeper slopes

and marginal areas, may have been done without appropriate soil and water conservation measures. Despite this increase, the agricultural productivity is following behind the population growth rate. On the other hand, the per capita land holding is also expected to decline from an average of 1.76 ha in 1985 to 0.66 ha in the year 2015 (IUCN, 1990).

However, most of the empirical evidences indicated that land use and land cover changes and socioeconomic dynamics have a strong relationship; as population increases the need for cultivated land, grazing land, fuel wood; settlement areas also increase to meet the growing demand for food and energy, and livestock population. Thus, population pressure, lack of awareness and weak management are considered as the major causes for the deforestation and degradation of natural resources in Ethiopia.

2.2. Effects of land use land cover on surface hydrology

Hydrologic responses to land use land cover changes and land management practices are the integrated indicators of the watershed conditions. A holistic understanding of the complex and dynamic land surface and its interacting parts is required to make precise predictions of the future water balance (Feyen et al., 2011). The rapid land cover change, coupled with climate variability could potentially lead to an increase in hydrologic impacts (Chen et al., 2013).

Quantitative assessment of the impact of climate and land cover changes on water resource availability is a significant issue for hydrological science (Shanshan et al., 2017). Knowledge of the distribution and types of land cover are essential for resource base analysis on land degradation, land productivity, and its impacts on water resources (Amsalu et al., 2007). Hence, comprehensive and improved procedures that integrate different techniques such as remote sensing, hydrologic modeling, and statistical approaches are necessary to identify the influence of land cover change and land management practices on the hydrological variability of a river basin.

Degraded watersheds tend to accelerate the overland flow, which reduces the soil moisture and groundwater recharge. Various studies used land cover mapping tools and methods to understand land cover changes, inventory of forest and natural resources as well as

understand the changes in the hydrologic behavior of watersheds (Mango et al., 2011; Kassa, 2009).

Investigating the impact of land cover land cover change on the hydrologic processes at sub basins level allows defining the degree of susceptibility of local water resources, and helps to plan appropriate mitigation measures that must be taken ahead of time. The impacts of agricultural land management practices and land cover change scenarios on the water balance are more evident at local sub basin scales; however, evidence for basin-scale impacts is limited (Schilling et al., 2020).

Land use land cover change is a major issue of concern with regards to change in the global environment (Qian et al., 2007). The rapid growth and expansion of urban centers, rapid population growth, scarcity of land, the need for more production, changing technologies are among the many drivers of land use land cover change in the world today (Barros, 2004).

The land use land cover plays a fundamental role in driving hydrological processes within a sub basin (Gwate et al., 2015). These include changes in water demands such as irrigation, changes in water supply from altered hydrological processes of infiltration, groundwater recharge, and runoff, and changes in water quality from agricultural runoff (DeFries et al., 2004). Therefore, a far better understanding of land use-cover change, its effect, and interaction to the hydrology of a basin is highly essential. Land use land cover changes respond to socioeconomic, political, cultural, demographic and environmental conditions and forces which are largely characterized by high human populations. Land use land cover change has become one of the major concern of researchers and decision makers around the world today. Therefore, a far better understanding of land use-cover change, its effect, and interaction to the hydrology of a basin is highly essential (Masek, 2009).

The human induced land use cover change impact mean that shifting in intent and/or management constitutes land use and land cover. It can also be dived into land use and land cover conversions, and land use and land cover modification. The physical conversion part refers to change from one cover or use type to another, as is the case in agricultural expansion, deforestation, or change in urban extent. Land use and land cover

modification, on the other hand, involves the maintenance of broad cover or use type in the face of change in its attributes. Both conversion and modifications of land use and land cover have important environmental consequences through their impacts on soil and water, biodiversity, and microclimate, hence, contribute to watershed degradation (Kassa, 2009).

Water resources are seriously affected by land use land cover dynamics. As the most direct expression of the interaction between human activities and the natural environment, land use land cover change is the interaction that links human activities and natural ecological processes (Zhang et al., 2014). Land use land cover changes directly affect the condition of water resources and agricultural economic growth. Land use/cover changes affect water resources mainly through vegetation interception, evapotranspiration, runoff, surface infiltration, soil moisture status, and so forth, thereby affecting the process of watershed hydrology and water resource cycles (Yao et al., 2014).

2.3. GIS and Remote Sensing Application

In most part of the world, land cover is dynamic, especially in rural and semi-rural areas. Under such condition, accurate, meaningful and availability of data on land is highly essential for planning and decision making. Among the various sources of land cover data, satellite remote sensing is particularly attractive. The importance of remote sensing was emphasized as a “unique view” of the spatial and temporal dynamics of the processes in land cover changes (Herold, 2003). Described that satellite remote sensing techniques have started to be used in 1970 s as a modern tools to detect and monitor land cover change at various scales with useful results.

Remote sensing (RS) is a powerful tool in deriving accurate and timely information on the spatial distribution of land use/land cover changes over large areas (Rogan, 2004) . GIS provides a platform for collecting, storing, analyzing and displaying digital data necessary for change detection (DeMers, 2008).

The change in land cover from rural to urban conditions and mapping of land cover establishes the baseline to predict to plan water resources, to monitor adjacent

environmentally sensitive areas, and to evaluate development, resource management, industrial activity, and/or reclamation efforts.

The vital component of mapping is to show the land cover changes in the watershed area and to divide land use in the various classes of land use. At this stage, remotely sensed imagery is of great help for obtaining information on temporal trends and spatial distribution of watershed areas and possible changes over the time dimension for projecting land cover changes but also to support changes impact assessment (Atasoy et al., 2006). Furthermore, multi temporal remotely sensed images are widely considered effective data sources that can be used to monitor the rapid changes of land cover, to classify types of land cover, and to obtain a timely regional overview of land cover information in a practical and economical manner over large areas.

GIS and remote sensing application tool is the most powerful tool in order to analyze and quantify soil erosion and sediment yield by using modified universal soil loss equation in addition to Soil and water assessment tool(SWAT).

2.3.1. ERDAS imagine and image classification

Remote sensed data provides the capability to monitor a wide range of landscape biophysical properties to management and policy, where information is needed in the past, present and future (Aspinall, 2008).

The image processing can broadly be categorized into: pre-processing, image classification or segmentation, post processing and evaluation (Jensen, 2004). The most common pre-processing techniques in remote sensing data include radiometric and geometric Correction, radiometric enhancement, spatial enhancement, spectral enhancement, and Fourier analysis (Jensen, 2004). Radiometric correction addresses variations in the pixel intensities (DNs) that are not caused by the object or scene being scanned. This correction aimed to minimize variation due to varying solar zenith angles and incident solar radiation.

Several algorithms have been developed to radiometric correction (Jensen, 2004). Land use land cover mapping and subsequent quantitative change detection required geometric

registration between TM and ETM scenes, and radiometric rectification to adjust for differences in atmospheric conditions, viewing geometry and sensor noise and response (Alemayehu, 2014). One of the pre-processing of satellite image is making geometric corrections before data base creation. Geometric correction addresses errors in the relative positions of pixels. It is undertaken to avoid geometric distortions from a distorted image.

There are many different approaches to classifying remotely sensed data. Image classification is the process of categorizing the pixels of an image into a specific number of individual classes based on set criteria (European Commission, 2001). Categorization is primarily based on the spectral patterns and radiance measurements obtained in the various bands of the individual pixels in an image (Alemayehu, 2014). However, in common image classification, there are two main classification namely unsupervised and supervised classification (Jensen, 2004).

Accuracy assessment is an essential and most crucial part of studying image classification and thus land use land cover change detection in order to understand and estimate the changes accurately. It is important to be able to derive accuracy for individual classification if the resulting data are to be useful in change detection analysis (Shewangizaw and Michael, 2010). This needs for accessing accuracy of spatial data derived from RS techniques and used in Geographic Information System (GIS) analysis has been recognized as a critical component of many projects. The most common accuracy assessment elements include overall accuracy, producer's accuracy, user's accuracy and kappa coefficient (Jensen, 2004).

One of the most common methods of expressing classification accuracy is the preparation of a classification error matrix (Lilleesand et al., 2004). An error matrix is an array of numbers set in rows and columns that express the number of sample units assigned to a particular category in one classification relative to the number of sample units assigned to a particular category in another classification (Ismail et al., 2009). The error matrices compare, on a category by category basis, the relationship between known reference data and the corresponding results of the automated classification. The matrix is able to identify both omission and commission errors in the classification as well as the overall, producer's and user's accuracy.

2.3.2. Unsupervised classification

In unsupervised classification, an algorithm is chosen that will take a remotely sensed data set and find a pre-specified number of statistical clusters in multi-spectral or hyper-spectral space (Ismail et al., 2009). The main purpose of unsupervised classification is to produce spectral groupings based on certain spectral similarities. In contrast to supervised classification, where we tell the system about the character (i.e., signature) of the information classes we are looking for, unsupervised classification requires no advance information about the classes of interest. Rather, it examines the data and breaks it into the most prevalent natural spectral groupings, or clusters, present in the data. The analyst then identifies these clusters as land cover classes through a combination of familiarity with the region and ground truth visits. The logic by which unsupervised classification works is known as cluster analysis.

2.3.3. Supervised classification

The first step in supervised classification is to identify examples of the information classes (i.e., land cover types) of interest in the image. These are called training sites. The software system is then used to develop a statistical characterization of the reflectance for each information class. This stage is often called signature analysis and may involve developing a characterization as simple as the mean or the range of reflectance on each band, or as complex as detailed analyses of the mean, variances and covariance's over all bands. Once a statistical characterization has been achieved for each information class, the image is then classified by examining the reflectance for each pixel and making a decision about which of the signatures it resembles most. There are several techniques for making these decisions, called classifiers. Most Image Processing software will offer several, based on varying decision rules.

Supervised classification does require prior knowledge of the ground cover in the study site. The supervised approach is preferred by most researchers because it generally gives more accurate class definitions and higher accuracy than the unsupervised classification (Ismail et al., 2009). Once trained, the algorithm can then be applied to the entire image and a final classification image is obtained. Supervised classification involves applying a

training process closely controlled by the analyst who must have good experience in the field (area of interest), because in this method the operator defines the spectral characteristics of the classes by identifying sample areas (training areas). The training samples (pixel representing known locations of the area being classified) are then used to classify the remainder of the images (Jensen, 2004).

Both the supervised and unsupervised classifications use the services of a classifier algorithm of which the maximum likelihood is the most popular (Lilleesand et al., 2004). Maximum likelihood is actually the probability that a pixel belonging to specific classes. It is a statistical decision rule that examines the probability function of a pixel for each of the classes, and assigns the pixel to the class with the highest probability and is perhaps the most widely used classification methods. It is one of the most popular methods of classification in RS and usually provides the highest classification accuracies (Ismail et al., 2009).

Supervised classification approach will select groups of training pixels that are representative for the six land cover units. This training data set forms the basis for classification of the total satellite image, by using the maximum likelihood classifier (MLC). In unsupervised classification approach, iso data clustering is commonly used, in which clusters of pixels based on their similarities in spectral information are automatically classified into the desired number of land use land cover categories.

2.3.4. Accuracy assessment and change detection

The importance of change detection is to determine which land-use class is changing to the other. The most commonly used land change detection methods include image overlay, classification comparisons of land cover statistics, change vector analysis, principal component analysis, image rationing and the differencing of normalized difference vegetation index (NDVI) (Han et al., 2009).

2.4. Hydrological models

Modeling of the rainfall-runoff processes of hydrology is needed for many different reasons. The main reasons being limited range of hydrological measurement techniques

and limited range of measurements in space and time (Beven, 2006). Therefore, it is necessary to develop a means of extrapolating from those available measurements in space and time to ungauged catchments and into the future to assess the likely impact of future hydrological changes. A wide range of hydrological models are used by the researchers, however, the applications of those models are highly dependent on the purposes for which the modeling is made.

According to Beven (2006) many rainfall-runoff models are carried out purely for research purposes as a means of enhancing knowledge about hydrological systems. He also added that other types of models are developed and employed as tools for simulation and prediction aiming ultimately to allow decision makers to improve decision making about hydrological problems. Before developing the hydrological models, it is very important to understand how the catchment responds to rainfall under different conditions.

On the basis of process description, the hydrological models can be categorized in to three main parts (Cundrelik, 2003).

1. Lumped models: - Parameters of lumped hydrologic models do not vary spatially within the basin and thus, basin response is evaluated only at the outlet, without explicitly accounting for the response of individual sub-basins. The parameters often do not represent physical features of hydrologic processes and usually involve certain degree of empiricism. These models are not usually applicable to event-scale processes. If the interest is primarily in the discharge prediction only, then these models can provide just as good simulations as complex physically based models (Cundrelik, 2003).

2. Distributed models: - Parameters of distributed models are fully allowed to vary in space at a resolution usually chosen by the user. Distributed modeling approach attempts to incorporate data concerning the spatial distribution of parameter variations together with computational algorithms to evaluate the influence of this distribution on simulated precipitation-runoff behavior. Distributed models generally require large amount of (often unavailable) data. However, the governing physical processes are modeled in detail, and if properly applied, they can provide the highest degree of accuracy (Cundrelik, 2003).

3. Semi-distributed models: - Parameters of semi-distributed (simplified distributed) models are partially allowed to vary in space by dividing the basin in to a number of smaller sub basins. The main advantage of these models is that their structure is more physically-based than the structure of lumped models, and they are less demanding on input data than fully distributed models. SWAT (Arnold, 1993), HEC (US-ACE, 2011), HBV (Bergström, 1995), are considered as semi-distributed models.

Hydrologic models can be further divided into event-based models, continuous-process models, or models capable of simulating both short-term and continuous events. Event based models are designed to simulate individual precipitation-runoff events. Their emphasis is placed on infiltration and surface runoff. Typically, event models have no provision for moisture recovery between storm events and, therefore, are not suited for the simulation of dry-weather flows. On the other hand, continuous-process models simulate instead a longer period, predicting watershed response both during and between precipitation events. They are suited for simulation of daily, monthly or seasonal stream flow, usually for long-term runoff-volume forecasting and for estimates of water yield (Cundrelik, 2003).

2.4.1. Brief description of few models

1. Soil and Water Assessment Tool (SWAT) Model: - Development of SWAT model is an ongoing process and it is the successor of “the Simulator for Water Resources in Rural Basins” model (SWRRB). SWAT model is a complex physically based model and was designed to test and forecast the water and sediment circulation and agriculture production with chemicals in ungauged basins. It is efficient in performing long term simulations.
2. Systeme Hydrologique European (MIKE SHE) Model: - It is a physically based model and hence it requires extensive physical parameters and was developed in 1990. The model accounts various processes of hydrological cycle such as precipitation, evapotranspiration, interception, river flow, saturated ground water flow, unsaturated ground water flow etc. It can simulate surface and ground water movement, their interactions, sediment, nutrient and pesticide transport in the model area and various water quality problems and can be applied for large watersheds.

3. Hydrologiska Byrans Vattenavdelning (HBV) Model: - This model is an example of semi distributed conceptual model (Bergstrom, 1976). The entire catchment is divided into sub catchments, which are further divided into different elevation and vegetation zones. It runs on daily and monthly rainfall data, air temperature and evaporation.
4. Hydrological Simulation Program-FORTRAN (HSPF) Model:- Hydrological Simulation Program-FORTRAN (HSPF) is a comprehensive, continuous watershed scale model developed by the United States Environmental Protection Agency for simulating many processes related to water quantity and quality in watersheds of almost any size and complexity. Values of many HSPF parameters can be conceived to index properties of specific factors that influence events such as water storage and fluxes in the land phase of the hydrologic cycle. Thus, one may categorize HSPF as moderately physically based model.

2.4.2. Model selection

The selection of a particular model is a key issue to get satisfactory answers to a given problem. Currently, there are numerous hydrological models simulating the hydrological process at different spatial and temporal scales. Although there are no clear rules for making a choice between models, some simple guidelines can be stated. Starting from the studied physical system, the first step is to define the problem and determine what information is needed and what questions need to be answered. This means that it is necessary to evaluate the required output, the hydrologic processes that need to be modeled, availability of input data. Subsequently the simplest method that can provide the answer to the questions has to be chosen. In particular it‘s necessary to identify the simplest model that will yield adequate accuracy, bearing in mind that model complexity is not synonymous with the accuracy of the results, that the model has to be characterized by flexibility, by the possibility of making it applicable under various spatial and temporal conditions and that increased accuracy has to be worth the increased effort.

There are a variety of criteria which can be used for choosing the right hydrological model for a specific problem. These criteria are project-dependent, since every project has its own specific requirements and needs. Further, some criteria are also user-dependent (and therefore subjective), such as the personal preference for graphical user interface,

computer operation system (OS), input-output (I/O) management and structure, or user's add- on expansibility. There are common and fundamental criteria to select a model according to (Cundrelik, 2003). These are model ability to explain past observation, ability to explain present observations, model ability to explain future observation, robustness or performance of the model to be applied in wide range condition and simplicity of the model for users.

2.4.3. Theoretical description of SWAT

The large scale spatial heterogeneity of the study area is represented by dividing the watershed into sub basins. Each sub basin is further discretized into a series of hydrologic response units (HRUs), which are unique soil-land use combinations. Soil water content, surface runoff, nutrient cycles, sediment yield, crop growth and management practices are simulated at each HRU and then aggregated for the sub basin by a weighted average. Physical characteristics, such as slope, reach dimensions, and climatic data are considered for each sub basin.

For climate, SWAT uses the data from the station nearest to the centric of each sub basin. Calculated flow, sediment yield, and nutrient loading obtained for each sub basins are then routed through the river system. Channel routing is simulated using the variable storage or Muskingum method. The water in each HRU in SWAT is stored in four storage volumes: shallow soil profile (0-2m), snow shallow aquifer (typically 2-20m), and deep aquifer. Surface runoff from daily rainfall is estimated using a modified SCS curve number method, which estimates the amount of runoff based on local land use, soil type, and antecedent moisture condition. Peak runoff predictions are based on a modification of the Rational Formula (Chow, 1988).

The watershed concentration time is estimated using Manning's formula, considering both overland and channel flow. The soil profile is subdivided into multiple layers that support soil water processes including infiltration, evaporation, plant uptake, lateral flow, and percolation to lower layers. The soil percolation component of SWAT uses a water storage capacity technique to predict flow through each soil layer in the root zone. Down ward flow occurs when field capacity of a soil layer is exceeded and the layer below is not

saturated. Percolation from the bottom of the soil profile recharges the shallow aquifer. Daily average soil temperature is simulated as a function of the maximum and minimum air temperature. If the temperature in a particular layer reaches less than or equal to 0°C, no percolation is allowed from that layer. Lateral sub-surface flow in the soil profile is calculated simultaneously with percolation.

2.4.4. SWAT Model Application on Land use Land cover change

The SWAT Model is one of the most widely used and scientifically accepted tool for assessing water quality, sediment transport and stream flow in a watershed; as evidenced by worldwide conferences and publications of SWAT related reports and articles. The use of the model is primary driven by the demand of various environmental agencies for direct and exploratory assessments of the impact of anthropogenic activities, climate change, and other wide range of land management issues on water and soil resources (Gassman et al., 2007). Since many watersheds globally are already experiencing degradation and calls for sound management of resources, SWAT has been increasingly used even outside of the United States of America. According to (Arnold et al., 2012) the SWAT model has also been used in countries such as China, Iran, Japan, Korea, Philippines, as well as countries in Europe and in Africa.

2.4.5. Hydrological Component of SWAT

The Simulation of the hydrology of a watershed is done in two separate divisions. One is the land phase of the hydrological cycle that controls the amount of water, sediment, nutrient and pesticide loadings to the main channel in each sub-basin. The second division is routing phase of the hydrologic cycle that can be defined as the movement of water, sediments, nutrients and organic chemicals through the channel network of the watershed to the outlet. In the land phase of hydrological cycle, SWAT simulates the hydrological cycle based on the water balance equation.

$$SWt = SWo + \sum_{i=1}^{t}(Rday - Qsuf - Ea - Wseep - Qgw) \quad \ldots\ldots\ldots\ldots\ldots (2.1)$$

Where: SWt is the final soil water content (mm), SWo is the initial soil water content on day i (mm), t is the time (days), Rday is the amount of precipitation on day i (mm), Qsurf is the amount of surface runoff on day i (mm), Ea is the amount of evapotranspiration on

day i (mm), Wseep is the amount of water entering the vadose zone from the soil profile on day i (mm), and Qgw is the amount of return flow on day i (mm).

1. Land phase of the hydrological cycle: - The main hydrological components simulated in the land phase of the hydrological cycle are evapotranspiration, lateral subsurface flow, groundwater flow, surface runoff, ponds, canopy storage, infiltration, redistribution, tributary channels, and return flow. SWAT simulates the land phase of the hydrological cycle based on the water balance equation (Neitsch et al., 2011).
2. Routing phase of the hydrologic cycle: - The second phase of the SWAT hydrologic simulation, the routing phase, consists of the movement of water, sediment and other constituents (e.g. nutrients, pesticides) in the stream network. The change in channel dimensions with time due to down cutting and widening is also included. Similar to the case for the overland flow, the rate and velocity of flow is calculated by using the manning's equation.

The main channels or reaches are assumed to have a trapezoidal shape by the model. Two options are available to route the flow in the channel networks: the variable storage and Muskingum methods. Both are variations of the kinematic wave model. The variable storage method uses a simple continuity equation in routing the storage volume, whereas the Muskingum routing method models the storage volume in a channel length as a combination of wedge and prism storages. While calculating the water balance in the channel flow, the transmission and evaporation are also well considered by the model. For this study, the variable storage method was adopted. The method was developed by (Williams, 1997) and recommended (Arnold et al., 1995).

CHAPTER THREE

MATERIALS AND METHODS

3.1. Description of the Study Area

3.1.1. Location

The Modjo watershed covers an area of 1,702 km^2 is located in the upper Awash River basin of Ethiopia. It lies within 8°35′00″N– 9°05′11″N and 38°54′35″E–39°15′30″E (Figure 3.1). The watershed is characterized by undulating topography with hills, mountains, plateaus, plains and river valleys.

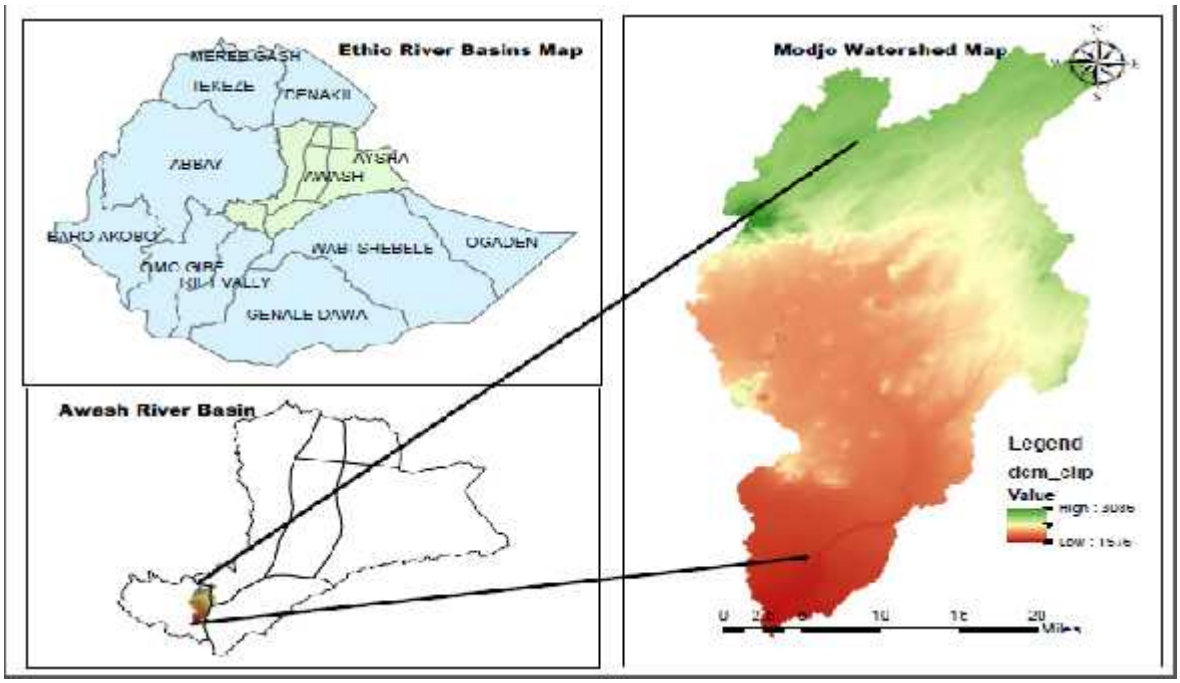

Figure 3. 1 Location map of Modjo watershed

3.1.2. Climate of the watershed

The study area is located within the main Ethiopian rift and mostly affected by the southerly and easterly. Indian Ocean air currents, as a result the air currents supply rain with bimodal characteristics. There are two main seasons in the study area, namely summer and winter also for locally called as Kiremt, Bega respectively. The main rainfall

season is summer season ends only four months from June to September. During this period the region receives the highest amount of rainfall as shown in Figure 3-2. The climate of Awash River Basin comes under the influence of the Inter-Tropical Convergence Zone (ITCZ).

The area has a bi-modal rainfall with a short rainy season from March to May and with a long rainy season from June to September. In the watershed the average monthly and annual scale rainfall patterns of the four selected stations were represented pictorially as Figure 3-2 and Figure 3-3 respectively. The average mean annual maximum temperature varies between 23·2°C and 27·9°C, whereas the minimum temperature varies from 10·6°C to 11·6°C. Maximum temperature values obtained in the months of May and minimum temperature was recorded in the month of August and it has generally been observed that the average annual temperature decreases with an increase in altitude.

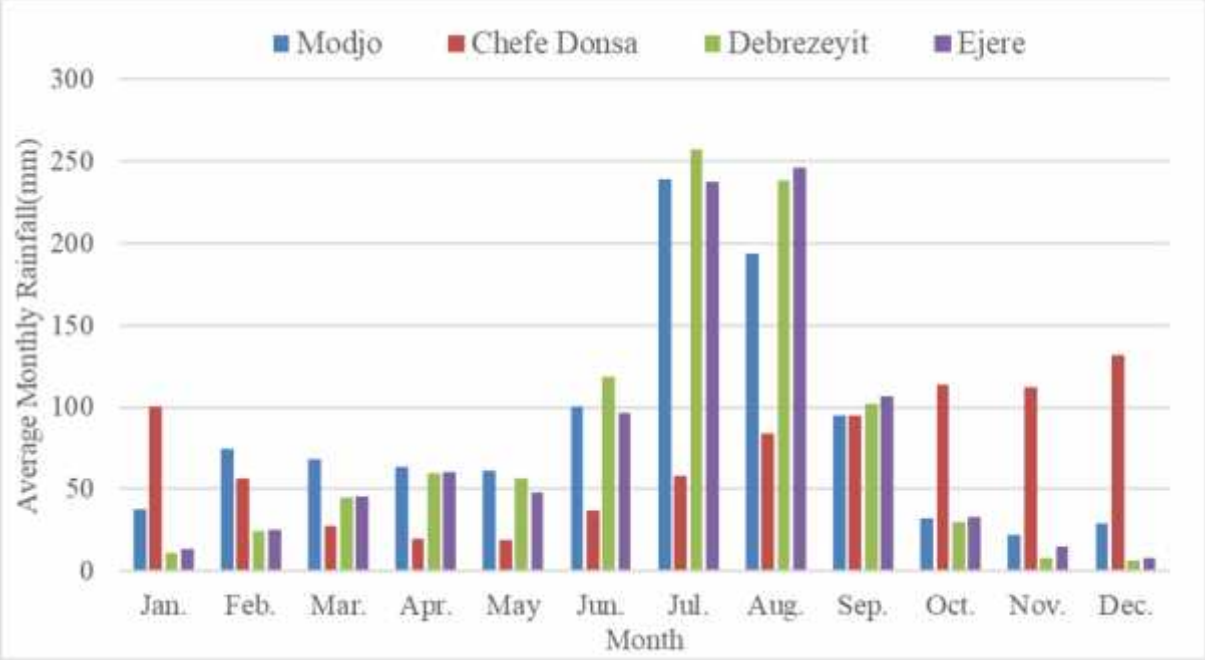

Figure 3. 2 Average monthly rainfall pattern of stations

3.1.3. Topography

Altitude in the basin increases from south to north and from west to east. The lowest point in the basin is located in the western edge and the highest in the north. The physiography of the watershed reveals a distinct variation with altitude that ranges from minimum elevation 1576 m above mean sea level (south of Modjo town) to maximum elevation 3073 m above mean sea level (at Yerer Volcanic ridges) and a Standard Deviation of 258.69m.

3.2. Materials used

Hydrologic modeling was done using Soil and Water Assessment Tool (SWAT) model. It is semi-distributed model which can be applied to model the impact of land management activities on water, sediment, nutrient etc. at watershed scale. It requires a certain input data which includes; weather, hydrological and spatial data.

Geographical Information System was used to process the spatial data and as interface to SWAT model. For this study GIS version 10.4 and SWAT 2012 was used. The Sequential Uncertainty Fitting, ver. 2 (SUFI-2) is one of the uncertainty analysis programs that is integrated in an independent program called SWAT Calibration and Uncertainty Program (SWAT-CUP) in order to carry out parameter and model uncertainties. The image classification was performed through Earth Resources Data Analysis System (ERDAS) Imagine 2014 software to generate the land use and land cover maps so as to detect the change in different categories of land use and land cover.

3.3. Model Input and Data Sources

3.3.1. Hydrological data

The Hydrological data was collected from Ministry of Water, Irrigation and Energy of Ethiopia. The flow data at Modjo gauging station was collected and arranged for the SWAT model analysis.

3.3.2. Weather data

Meteorological datas needed by the SWAT model to simulate the hydrological conditions of the basin were collected from National Meteorological Agency of Ethiopia, Adama

National Meteorology Agency branch and Awash Melkassa Research Institution. The meteorological data like precipitation, maximum and minimum temperature, relative humidity, and wind speed and sunshine hours from four stations on the watershed were used (Debrezeyit, Ejere, Chefe-Donsa and Modjo) for the years 1989 -2018.

3.3.3 Soil properties and Soil map

The soil map has been referenced with FAO (1998) world soil database to obtain the physical properties of the individual soils. The properties of the soils are mainly parameters related to soil texture and grain size percentage composition which is helpful to compute other necessary physical soil characteristics. Apart from the properties of the soils obtained from FAO (1998) soil map, additional soil characteristics are required to set up SWAT model. Soil saturated hydraulic conductivity, bulk density, soil available water and texture class at different soil depths are crucial for modeling with SWAT.

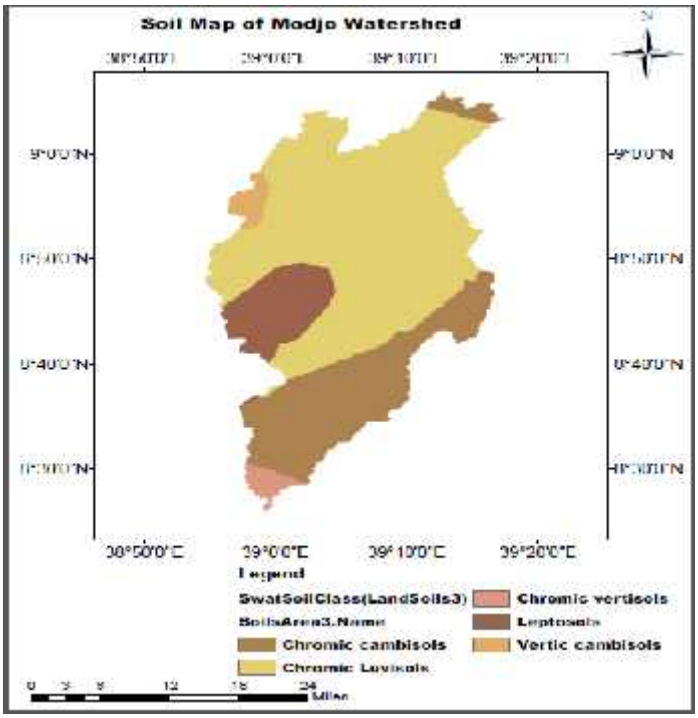

Figure 3. 3 Soil Map of Modjo watershed

Soil of Ethiopia is not available in SWAT data bases. The compared properties of Ethiopian soils with the SWAT data base soils then edit and represent with it in the look up table. Chromic Luvisols (60%) followed by Chromic Cambisols (25.29%), Leptosols

(10.00%), Vertic Cambisols (2.00%) and Chromic Vertisols (1.76%) are the major dominant soil types of the watershed.

3.3.4 DEM

Digital Elevation Model (DEM) data is required to calculate the flow accumulation, stream networks, and watershed delineation using SWAT watershed delineator tools. A 30 m by 30m resolution ASTER Global Digital Elevation Model was obtained from the NASA website. This data was projected to Transverse Mercator (UTM) on spheroid of WGS84 and it was in raster format to fit in to the model requirement (Figure 6).

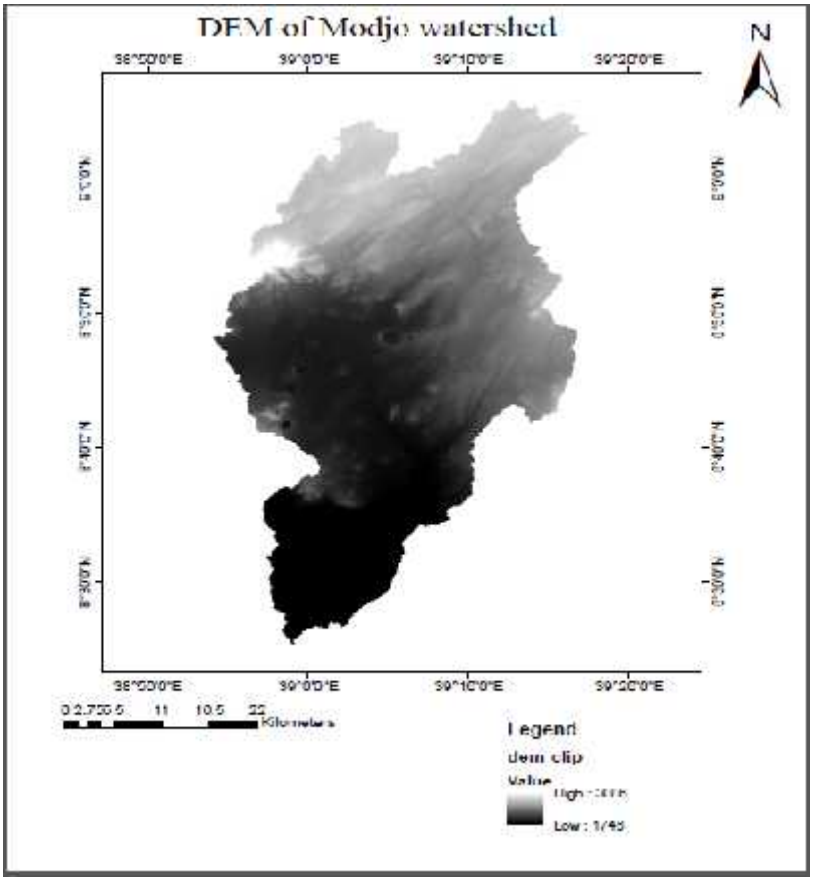

Figure 3. 4 DEM of Modjo watershed

3.3.5 Land use land cover map

Land use is the most important factors that affect runoff, evapotranspiration and surface erosion in a watershed. This data required by SWAT model to describe the Hydrological Response Units (HRUs) of the watershed together with slope and soil map.

The SWAT model has predefined land use categories in its database. To make compatible with it lookup table was prepared which includes the corresponding land use categories of the model for each land use categories of the watershed. The land use and land cover classification was made using land sat imageries downloaded from http://glovis.usgs.gov/ website.

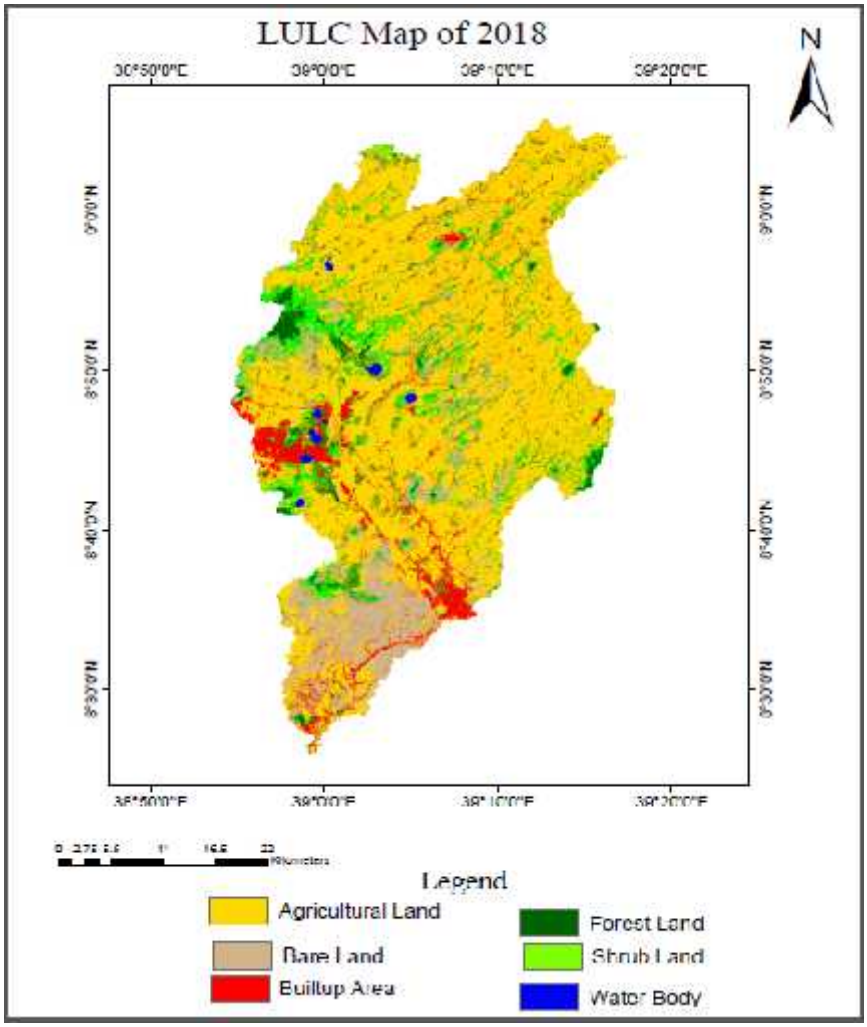

Figure 3. 5 Land use land cover map of Modjo watershed

3.4. Hydrological Component of SWAT Hydrologic modeling

3.4.1. Land phase of Hydrologic cycle in SWAT

3.4.1.1. Surface runoff/overland flow

Surface runoff occurs whenever the rate of water application to the ground surface exceeds the rate of infiltration (Neitsch et al., 2011). When water is initially applied to a dry soil, the infiltration rate is usually very high. However, it will decrease as the soil becomes wetter. When the rate of application is higher than the infiltration rate, surface depressions begin to fill. If the application rate continues to be higher than the infiltration rate once the all surface depressions have filled, surface runoff will commence (Neitsch et al., 2011). SWAT provides two methods for estimating the surface runoff: the SCS curve number procedure (SCS, 1972) and the Green and Ampt infiltration method (Green and Ampt, 1911).

The SCS curve number is a function of the soil's permeability, land use and antecedent moisture conditions (SCS, 1972) whereas the Green and Ampt infiltration method calculates infiltration as a function of the wetting front metric potential and effective hydraulic conductivity (Green and Ampt, 1911). SWAT uses the daily and hourly time steps to calculate surface runoff. For daily time steps, SWAT uses an empirical SCS curve number (CN) method and for hourly time steps SWAT uses the Green and Ampt equation.

For this project the SCS curve number was adopted for the simulation of surface runoff in SWAT since it requires the readily available daily data that can be obtained from easily from government ministries and/or offices. The SCS curve number equation is (SCS, 1972):

$$Qsurf = \left(\frac{(R_{day} - I_a}{(Rday - Ia + S)} \right) \quad \ldots 3.1$$

Where, Q surf is the accumulated runoff or rainfall excess (mm H2O), Rday is the rainfall depth for the day (mm H2O), I = initial abstraction (mm), S = retention parameter (mm)

The retention parameter (S) is defined as:

$$S = 25.4\left(\frac{1000}{CN} - 10\right) \quad \ldots 3.2$$

Where, CN is the curve number for the day

To compute the surface runoff depth using the above stated equation 3-4, CN is the major parameter to be used in the SWAT model. The SCS curve number is a function of the soil's permeability, land use and antecedent moisture conditions: 1-dry (wilting point), 2- (average moisture), and 3- wet (field capacity). The moisture condition 1, curve number is the lowest value that the daily curve number can assume in dry conditions. The curve numbers 2 and 3 are calculated from equations below.

$$CN_1 = CN_2 - \frac{20 * (100 - CN_2)}{(100 - CN_2 + \exp(2.533 - 0.0636 * (100 - CN_2)} \quad \ldots 3.3$$

Where, CN1 is the moisture condition 1 curve number, CN2 is moisture condition 2 curve numbers, and CN3 is the moisture condition 3-curve number (Neitsch et al., 2011).

The initial abstractions, Ia, is commonly approximated as 0.2S and the above equation above becomes:

$$Q_{surf} = \frac{(R_{day} - I_a)^2}{(R_{day} + 0.8S)} \quad \ldots 3.4$$

Referring to the above equations, runoff will occur when $R_{day} > I_a$. Therefore, there is some amount of rainfall Ia (initial abstraction before ponding) for which no runoff will occur (i.e., runoff is zero) (Chow et al., 1998). The peak runoff rate is the maximum is the maximum runoff rate that occurs with a given rainfall event (Neitsch et al., 2011).

The peak runoff rate is an indicator of the erosive power of a storm and is used to predict sediment loss. SWAT uses a modified rational method to calculate the peak runoff rate.

$$q_{peak} = \frac{\alpha_k Q_{surf} Area}{3.6 t_{conc}} \quad \ldots 3.5$$

Where, q_{peak} is the peak runoff rate (m^3 / s), α_k is the fraction of daily rainfall that occurs during the time of concentration, Qsurf is the surface runoff (mm), Area is the sub basin area (km^2),t_{conc} is the time of concentration for the sub basin (hr) and 3.6 is a unit conversion factor.

3.4.1.2. Potential Evapotranspiration

Potential Evapotranspiration is a collective term that includes evaporation from the plant (transpiration) and evaporation from the water bodies and soil. Evaporation is the primary mechanism by which water is removed from a watershed. An accurate estimation of evapotranspiration is critical in the assessment of water resources and the impact of land use change on these resources.

There are many methods that are developed to estimate potential evapotranspiration (PET). SWAT provides three options for PET calculation: Penman-Monteith (Monteith, 1965), Priestley-Taylor (Priestley and Taylor, 1972), and Hargreaves (Hargreaves et al., 1985) methods. The methods have various data needs of climate variables. Penman-Monteith method requires solar radiation, air temperature, relative humidity and wind sped; Priestley-Taylor method requires solar radiation, air temperature and relative humidity; whereas Hargreaves method requires air temperature only.

For this study, the Penman-Monteith method was selected as the method is widely used and all climatic variables required by the model are available for the three stations in and around the study watershed area.

3.4.2. Routing phase of Hydrologic cycle in SWAT

The second component of the simulation of the hydrology of a watershed is the routing phase of the hydrologic cycle. It consists of the movement of water, sediment and other constituents (e.g. nutrients, pesticides) in the stream network.

Two options are available to route the flow in the channel network: the variable storage and Muskingum methods. The variable storage method uses a simple continuity equation in routing the storage volume, whereas the Muskingum routing method models the storage volume in a channel length as a combination of wedge and prism storages. In the latter

method, when a flood wave advances into a reach segment, inflow exceeds outflow and a wedge of storage is produced. As the flood wave recedes or retreat, outflow exceeds inflow in the reach segment and a negative wedge is produced. In addition to the wedge storage, the reach segment contains a prism of storage formed by a volume of constant cross-section along the reach length.

The variable storage method was used for this study. The method was developed by (Williams, 1969). The equation of the variable storage routing is given by:

$$\Delta V_{stored} = V_{in} - V_{out} \quad \ldots 3.6$$

Where, ΔVstored is the change in volume of storage during the time step (m^3 water), Vin is the volume of inflow during the time step (m^3 water), and Vout is the volume of outflow during the time step (m^3 water).

3.4.3 Soil Erosion and Sediment Estimation

Modjo watershed has one river discharge gauging station, which is located in the west of Modjo town. Measured daily discharge data between 1989 and 2018 was used to validate the model Output. SWAT calculates sediment yields resulting from surface runoff and soil erosion by using Modified Universal Soil Loss Equation (MUSLE) (Neitsch et al., 2011). The integrated MUSLE was used to estimate sediment yield of the catchment:

$$Sed = 11.8(Qsurf * Qpeak * Areahru)^{0.56} * K * CUSLE * P * L * CFGR \ldots (3.7)$$

Where, Sed is the sediment yield on a given day (metric tons), Qsurf is the surface runoff volume (mm /ha), $Q_{peak}$is the peak runoff rate (m^3/s), $Area_{hru}$is the area of the HRU (ha), K is the soil erodibility factor from the Nomograph. C_{USLE} is the cover and management factor, P is the support practice factor, L is the topographic factor and CFRG is the coarse fragment factor.

Sediment data which is collected from Ministry of Water, Irrigation and Electricity (MoWIE) is not in continuous time step which means collect sediment samples were collected and calculated the sediment concentration per three months. Therefore, it is

necessary to generate the continuous sediment load by relating the stream flow with sediment load using sediment rating curve.

Sediment rating curve: a sediment-rating curve expresses the average relation between discharge and suspended sediment concentration for a certain location. The sediment rating curve was calculated by the following formula (Horowitz, 2003).

$$Qs = aQ^b \quad \ldots (3.8)$$

Where, Qs is the suspended sediment transport (M tons/day)

Q is water discharge (m^3/s)

a and b are regression coefficient and exponent, respectively.

The total sediment discharge in tons/day is the multiplication of the flux-averaged total sediment concentration, the daily mean water discharge, and a conversion factor (Julien PY , 1998).

$$S = 0.0864 * Q * C \quad \ldots (3.9)$$

Where, S is sediment load in (t/day),

Q is streamflow (m^3/s),

C is sediment concentration (mg/l) and 0.0864 is conversion factor.

3.5. Data Preparation

Data preparation to the required model input is important and has influences on the model output. The relevant time series data used for this study included daily rainfall data, stream flows, sediment data, temperature (minimum and maximum), relative humidity, wind speed and solar radiation.

3.5.1. Filling missing data

The inverse distance (reciprocal-distance) weighting method (IDWM) (Wei et al., 1973) is the method commonly used for estimating missing data. This weighting distance method for estimating the missing value of an observation, which uses the observed values at other stations, was determined by the following Equation.

$$Vo = \frac{\sum_{i=1}^{n} \frac{Vi}{Di}}{\sum_{i=1}^{n} \frac{1}{Di}} \quad \ldots (3.10)$$

Where, V_0 is the estimated value of the missing data, V_i is the value of the same parameter at i^{th} nearest weather station; D_i is the distance between the station with missing data and the i^{th} nearest weather station.

3.5.2. Consistency

Double Mass Curve (DMC) was used to check the consistency of rainfall for adjustment of inconsistent data. This technique was based on the principle that when each recorded data comes from the same parent sample, they are consistent. A group of 4 base stations in the neighborhood of the station were selected.

A double-mass curve is a graph of the cumulative annual precipitation of group stations versus the cumulative mean annual precipitation of selected stations of one or more gauges in the region that has been subjected to similar hydro meteorological occurrences and is known to be consistent. If a rainfall record is a consistent estimator of the hydro meteorological occurrences over the period of record. A change in the slope of the double mass curve would suggest that an external factor has caused changes in the character of the measured values. If a change in slope is evident, then either the record needs to be adjusted with the early or the later period of record adjusted.

A group of base stations in the neighborhood of the station were selected and checked by using equation 3.11.

$$Px = \frac{1}{n} * \left(\left(\frac{Nx}{N1} \right) * P1 + \left(\frac{Nx}{N2} \right) * P2 + \cdots + \left(\frac{Nx}{Nn} \right) * Pn \right) \quad \ldots (3.11)$$

Where, P_x is the missing data at station x, Nx is the missing data stations normal annual rainfall, Ni is normal annual rainfall at station i, and n is number of nearby gauges The station-average method for estimating missing data uses n gauges from a region to estimate the missing point rainfall, PX, at another gauge.

The double-mass curve for checking the consistency of precipitation records is explained by Figure 3.6 in which the annual records of four meteorological stations. These are Chefe

Donsa, Debrezeyit, Ejere and Modjo. The cumulative precipitation for each station was plotted against the cumulative precipitation of the group station. According to the double mass curve (Figure 3.6) graph the hydrological data were found consistently.

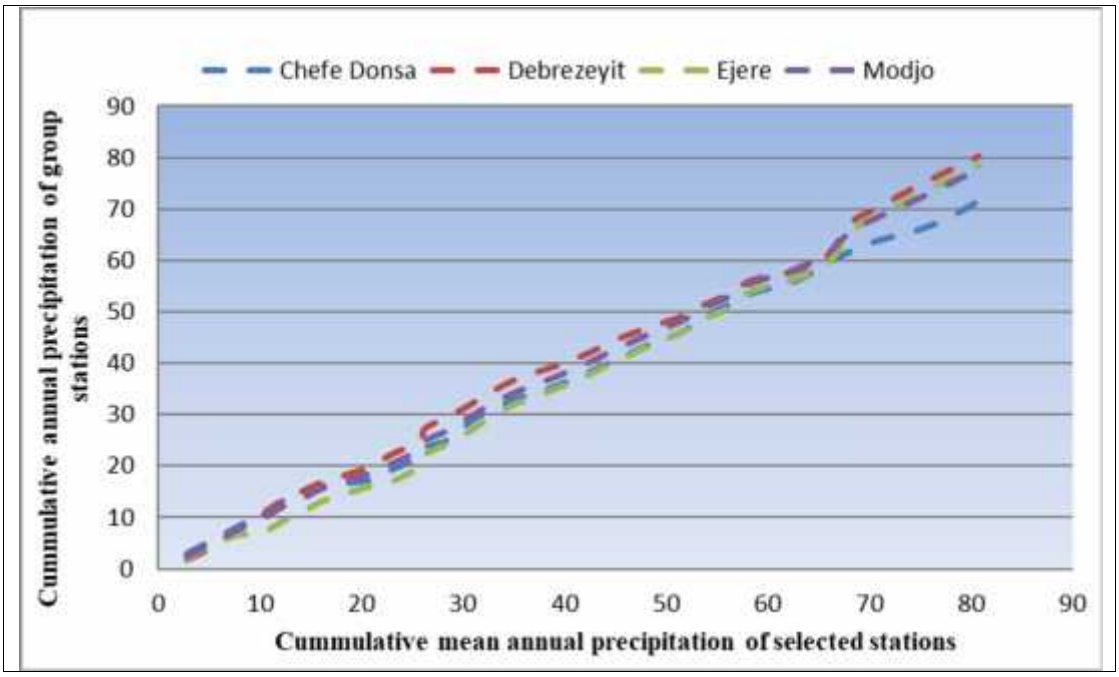

Figure 3. 6 Double mass curve for selected stations

3.5.3. Homogeneity test

Frequency analysis of rainfall data requires that the data be homogeneous and independent. The restriction of homogeneity assures that the observations are from the same population. One of the test of homogeneity (Buishand, 1982) is based on the cumulative deviations from the mean:

$$S_k = \sum_{i=1}^{k} (X_i - \bar{X}) \qquad \ldots (3.12)$$

Where Xi are the records from the series X1, X2… X_n and $\bar{X}$ the mean. The initial value of S_k=0 and last value S_k=n are equal to zero (Figure 3.7).

In order to test the rainfall homogeneity, the homogeneity of the stations were made by the rainbow model (Figure 3.7). When the deviation crosses one of the horizontal lines the homogeneity of the data set is rejected with 90, 95 and 99% probability (Raes, 1996). As

shown in Figure 3.7 the deviation of the selected station was not crossed the horizontal line. Therefore, the data series is considered as homogeneous. Therefore, annual rainfall time series over the period 1989-2018 at four meteorological stations located in Modjo watershed was assessed and they can be used for this particular study.

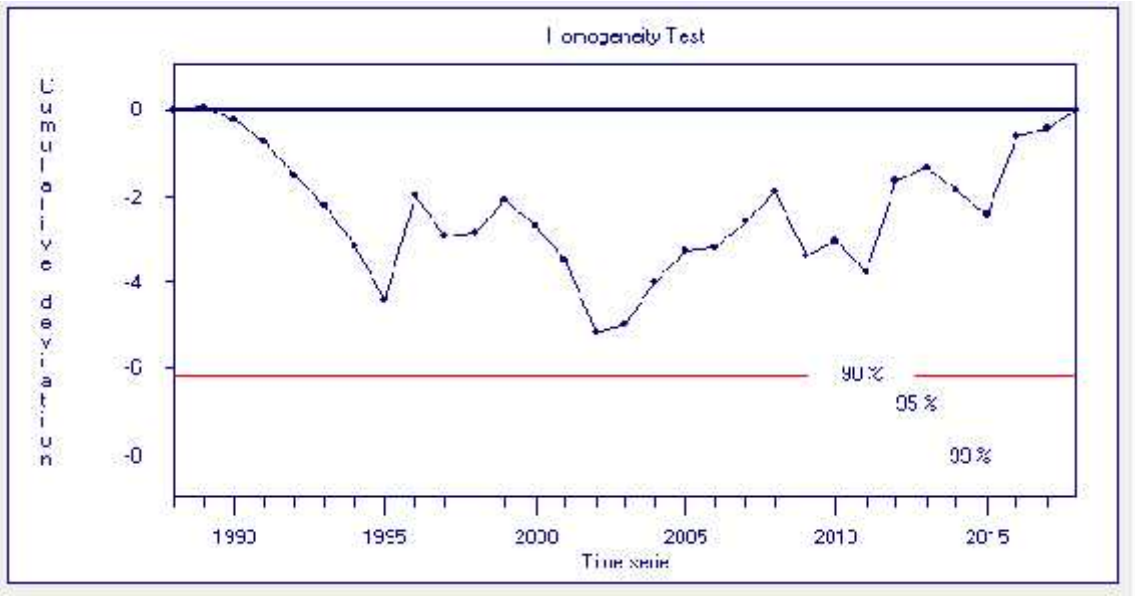

Figure 3. 7 Homogeneity test for selected stations

3.6. Land use land cover analysis

SWAT Model has defined or established previously land use categories in its data sets and then land use and land cover change detection was analyzed for the 30 years in GIS. In order to implicate the change differences in the watershed Imageries of different Land Sat Thematic Mapper was downloaded in path 168 and Row 054 at a spatial resolution of 30 m from the United State Geological Survey (USGS) earth explorer in Geo (http://glovis.usgs.gov/website) TIFF format. Land use cover maps of 1989, 1999, 2009 and 2018 were used in this study. After the imagery was downloaded the following major process was carried out for land use land cover detection. Image processing, image classification and accuracy assessment were major processes under taken.

3.6.1. Image processing

Satellite image pre-processing before change detection phenomenon is very important in order to establish a more direct affiliation between the acquired data and biophysical

phenomena (Tolera et al., 2018). Due to acquisition system and platform movements, remotely-sensed data from satellites are generally geometrically distorted. The satellite data were imported into ERDAS 2014 software in an image format for geometric correction.

In this research, geometric, radiometric, and atmospheric corrections were applied to remove image noise. Then, layer stacking and image sub-setting were conducted. Land sat imageries were used to change detection of land use and land cover in the Modjo watershed from 1989 to 2018. Land sat 5, 7 and 8 Thematic Mapper (L5, 7 and 8 TM) was used for data acquisition. To avoid a seasonal variation in vegetation pattern and distribution throughout a year, the selection of dates of the acquired data were made in the same annual season of the acquired years.

The images used in this study area were geo-referenced to a Universal Transverse Mercator projection using datum WGS (World Geodetic System) 84 zone 37N prior to image classification. So as to view and distinguish the surface features clearly, all the input satellite images were composed using the RGB color composition. The images provide complete coverage of Modjo watershed. The raw image acquisition dates, cloud cover and path/row of the satellite images used in this study are summarized under the following table.

Table 3. 1 The acquisition dates and path/row of the images

Path/Raw	Acquisition date	cloud cover
168 / 054	Jan-29- 1989	0.00
168 /0 54	Dec -03- 1999	0.00
168 /0 54	Jan -12-2009	1.00
168 /0 54	Jan- 17- 2018	1.00

3.6.2. Image Classification

There are two types of image classification approaches in ERDAS Imagine; these are unsupervised and supervised image classification. To collect the training sites ERDAS imagine 2014 was linked with Google earth.

Table 3. 2 Land use land cover classes and their definitions

Land use land cover Classes	Definitions
Agricultural Land	Agricultural Land may be defined broadly as land use primarily for production of food and fiber.
Shrub Land	The typical shrub occurrences are found in those arid and semi-arid regions characterized by xerophytic vegetative types.
Forest	Forest lands have a tree-crown areal density (crown closure percentage) of 10% or more, are stocked with trees capable of producing timber or other wood products, and exert an influence on the climate or water regime.
Bare Land	Barren Land is land of limited to support life and in which less than one –third of the area has vegetation or other cover.
Built-up	Built-up land is comprised of areas of intensive use with much of land covered by cities, towns, structures, high ways, transportation, power and communication.
Water Body	The delineation of water areas depend on the scale of data presentation and the scale and resolution of characteristics of the remote sensor data used for interpretation of land use and cover.

Supervised Image classification was carried out by using the maximum likelihood classifier algorithm. The study area was classified into six major classes to perform different classification techniques based on the most located features into the study area to obtain the thematic maps of land use and land cover. These are agricultural land, shrub land, forest, bare land, built-up and water body.

3.6.3. Accuracy assessment

The accuracy is typically used to express the degree of correctness of a classification result and the final step of the satellite image classification. Supervised classification algorithm

with maximum likelihood classifier in the form of Error matrix was applied to the collected imagery in order to perform imagery classification to map the land use land cover theme of Modjo watershed.

The accuracy assessment and statistical analysis of the expected results were conducted to get an accurate and suitable approach to classify the study area of this research. Tabular output reports on Appendix section (Appendix B, C, D and E), respectively which include value of Producer accuracy, user accuracy, over all accuracy and kappa statistics were described under the result and discussion section.

$$K = \frac{P_o - P_c}{1 - P_c} \qquad \ldots(3.13)$$

Where; K is kappa statistics, P_o is proportion of correctly simulated cell and P_c is expected proportion correction by chance between observed and simulated. K=1-perfect, K≤ 0.5-rare, 0.5 ≤ K ≤ 0.75-medium and 0.75≤ K ≤ 1-high level of agreement.

3.7 Hydrological Modeling

3.7.1. SWAT model overview

SWAT uses spatially distributed data on topography, soils, land cover, land management, and weather to predict water, sediment, nutrient, pesticide, and fecal bacteria yields. In the current versions, a modeled watershed is divided spatially into sub watersheds using digital elevation data according to the density specified by the user.

Sub watersheds are further subdivided into lumped, non-spatial hydrologic response units (HRUs) consisting of all areas within the sub watershed having similar landscape characteristics. Versions 2000 and earlier model sub watersheds as having uniform slope and climatic conditions, and HRUs as having similar soil, land use, and land management characteristics. Versions 2005 and 2009 allow slope to be included at the HRU level.

SWAT model was selected for the analysis of stream flow and sediment yield by the following reasons; the model was applied for similar study in different parts of the world

simulates the most important hydrological process in the watersheds, it is less demanding on input data, and it is readily and freely available.

3.7.2. SWAT model input Data

SWAT model requires spatial data and temporal data. Spatial data include a digital elevation model (DEM), land-use map and soil map was obtained from the Ministry of Water, Irrigation and Energy (MoWIE) of Ethiopia. The soil map has been referenced with FAO (1998) world soil database to obtain the physical properties of the individual soils.

The temporal data include hydrological data (stream flow & sediment yield) and climatic data (precipitation, solar radiation, relative humidity, wind speed and temperature). Within SWAT, a catchment is divided into multiple sub-catchments which are then further divided into Hydrologic Response Units (HRUs) that consist of homogeneous land use, slope and soil characteristics.

3.7.3. SWAT model Setup

3.7.3.1. Watershed Delineation

The watershed boundary was divided into different sub-watershed and sub-watershed was into HRUs to allow spatially detailed simulation by reflecting differences in various hydrological conditions for different LULCs, soils and slope configurations. The watershed delineation interface in Arc SWAT was separated into five sections including DEM Set Up, Stream Definition, Outlet and Inlet Definition, Watershed Outlet(s) Selection and Definition and Calculation of Sub basin parameters. In order to delineate the networks sub basins, a critical threshold value was required to define the minimum drainage area required to form the origin of a stream. The whole watershed was divided in to 29 sub-basins.

After the initial sub basin delineation, the generated stream network can be edited and refined by the inclusion of additional sub basin inlet or outlets. Adding an outlet at the location of established monitoring station is useful for the comparison of flow concentrations between the predicted and observed data. Therefore, one sub basin outlet

was manually edited into the watershed based on known stream gage location that has sufficient stream flow data available from 1989-2018.

3.7.3.2. HRU Definition

The SWAT (Arc View version) model requires the creation of Hydrologic Response Units (HRUs), which are the unique combinations of land use and soil type within each sub basin. A combination of Land use area over the sub-basin, soil class over the land use, and slope class over the soil was done for HRU definition for the study area. The reclassified land use and soil was overlaid with slope class.

HRU analysis in Arc SWAT includes divisions of HRUs by slope classes in addition to land use and soils. The multiple slope option (an option for considering different slope classes for HRU definition) was selected for this study. Which were classified into four classes (namely 0-5%; 5-10%; 10-15% and 15-20%) Slope classification was carried out based on the elevation range of the DEM used during watershed delineation.

The SWAT user's manual suggests that a 5 % land use threshold, 10 % soil threshold and 10 % slope threshold are adequate for most modeling application. Hence, the Modjo watershed was divided in to different HRUs; each has a unique combination land use, slope and soil. The slope values of the watershed were reclassified in percent. It reclassified in to four classes as shown in the Table 3-2.

Table 3. 3 The slope classes used

Classes	Slope range (%)
Class 1	0-5
Class 2	5-10
Class 3	10-15
Class 4	15-20

3.7.3.3. Watershed Data Definition

SWAT requires long year's daily record of precipitation, maximum and minimum temperature, solar radiation, relative humidity and wind speed. These data records and geographic locations were prepared according to the model table format and saved in DBF format (batch file) so as to import in to the database by using weather data input wizard. Values for all these variables can read from records of observed data or they may be generated by using weather generator station.

The SWAT Model contains weather generator model called WXGEN (Shapley and Williams, 1990). It was used in SWAT model to generate climatic data or to fill missing data using monthly statistics which is calculated from existing daily data. In this study, weather generator parameters were estimated using 30 years of measured records. The weather generator input file contains the statistical data needed to generate representative daily climate data for the sub basins.

3.8. SWAT model sensitivity analysis, calibration and validation

3.8.1. Sensitivity Analysis

Sensitivity analyses can be global, which attempts to assess all combinations of all parameter values, or local, which evaluates a specific set of parameters one at a time while the remaining parameters are fixed. Global and local methods may yield different results because of how they select and prioritize parameters (Arnold et al., 2012). Global sensitivity analysis uses t-stat and p-values to determine the sensitivity of each parameter. The t-stat provides a measure of the sensitivity (larger in absolute values are more sensitive) and the p-values determine significance of the sensitivity. A p-value close to zero has more significance (Abbaspour et al., 2015).

After the model setup has been finished, the next step is to run the model and analyze the simulation result. Sensitivity analysis is used to estimate the rate of change of model outputs with respect to change of model inputs. It is also useful to recognize how the model depends on the information fed into it (Willems, 2000). Sensitivity analysis provides for better understanding of the behavior of the system being modeled, such as model parameters and applicability, thus it increases the confidence level of the model and its predictions. SWAT model have large number of parameters and a number of outputs,

thus, an initial parameter selection makes the calibration process easier and reduces the uncertainties related to diverse parameters.

3.8.2. Calibration and Validation

Model calibration is a process in which a generalized model is adjusted so that the model predictions better represent site specific hydrologic processes and conditions. During calibration, model parameters are optimized in an effort to increase accuracy and reduce model prediction uncertainty. Calibration is performed by carefully selecting model parameter values, adjusting them within their recommended ranges, and comparing predicted output variables with observed data for a given set of conditions (Arnold et al., 2012).

Automatic calibration and uncertainty analysis incorporated in SWAT2012 via the SWAT-CUP (SWAT Calibration and Uncertainty Procedures) software developed and tested (Abbaspour, 2012) with the semi-automated program SUFI2 (Sequential Uncertainty Fitting ver. 2) was used for this study. Prior to model calibration parameter sensitivity analysis was done using the SUFI2 global sensitivity methods, for the whole catchment area. Therefore, in this study the hydrologic component of the model was calibrated at Modjo gauging station in order to make the simulation result more realistic for independent calibration period. River discharge data of 1989 to 2008 was used to calibrate the SWAT model.

Uncertainties can be quantified in SUFI-2 by a measure of P - factor and R - factor. The P-factor is the percentage of measured data bracketed by 95PPU or 95% prediction uncertainty According to (Abbaspour, 2014). Whereas, R- factor is the average thickness of the 95PPU band divided by the standard deviation of the measured data. It means R-factor measures the strength of uncertainty analysis and calibration. When simulation matches with the observed, the resulting value of R- factor close to zero and P- factor close to 1 and it indicates a low level of uncertainty has contained in the simulation.

A warm-up period of 2 years (1988-1990) was used for model initialization during the model calibration. Validation was performed to compare the model outputs with an

independent data set without making further adjustment of the parameter values. River discharge data of 2009-2018 was used to validate the SWAT model.

In this study 12 flow parameters were considered in the calibration process. First, some sensitivity flow parameters were adjusted by manual calibration procedure based on the available information in literatures. Consequently, adjustment was done for other sensitive parameters. The model was run using the best parameter output values and the simulations were compared with observed stream flow data using Percent BIAS (PBIAS), Nash and Sutcliffe coefficient of efficiency (NSE) and coefficient of determination (R^2).

3.9. Model Performance Evaluation

The model performance in predicting the catchment condition was evaluated using of the statistical analysis parameters such as coefficient of determination (R^2) and Nash Sutcliffe efficiency (NSE), percent bias (PBIAS) and root mean square error standard deviation ratio (RSR). The ArcSWAT model for stream flow and sediment transport simulation at daily and monthly time steps during calibration and validation periods was rigorously evaluated using statistical indices. Table in the Appendix A shows the performance ratings for different statistical indices, R^2, NSE and PBIAS, as suggested by (Moriasi et al., 2007).

$$R^2 = \frac{\left[\sum_{i=1}^{n}\left(X_i^{obs} - X_{mean}^{obs}\right)\left(Y_i^{sim} - Y_{mean}^{sim}\right)\right]^2}{\sum_{i=1}^{n}\left(X_i^{obs} - X_{mean}^{obs}\right)^2 \sum_{i=1}^{n}\left(Y_i^{sim} - Y_{mean}^{sim}\right)^2} \quad \ldots (3.14)$$

Where, Xi – measured value

Yi – simulated value and

Xmean– mean measured value and Ymean-mean simulated value

$$NSE = 1 - \left[\frac{\sum_{i=1}^{n}(X_i^{obs} - X_i^{sim})^{\wedge 2}}{\sum_{i=1}^{n}(X_i^{obs} - X_i^{mean})^{\wedge 2}}\right] \quad \ldots (3.15)$$

Where, Xi – measured value
Yi – simulated value and
Xav – average observed value

$$RSR = \frac{\sqrt{\sum_{i=1}^{n}\left(X_i^{obs} - Y_i^{sim}\right)^2}}{\sqrt{\sum_{i=1}^{n}\left(X_i^{obs} - Y_i^{obs}\right)^2}} \quad \ldots (3.16)$$

Where, Xi – measured value (m^3/s)
Yi – simulated value (m^3/s)

$$PBIAS = \left[\frac{\sum_{i=1}^{n}\left(Y_i^{obs} - Y_{i=1}^{sim}\right) * 100}{\sum_{i=1}^{n} Y_i^{obs}}\right] \quad \ldots (3.17)$$

Where, Xi – measured value
Yi – simulated value

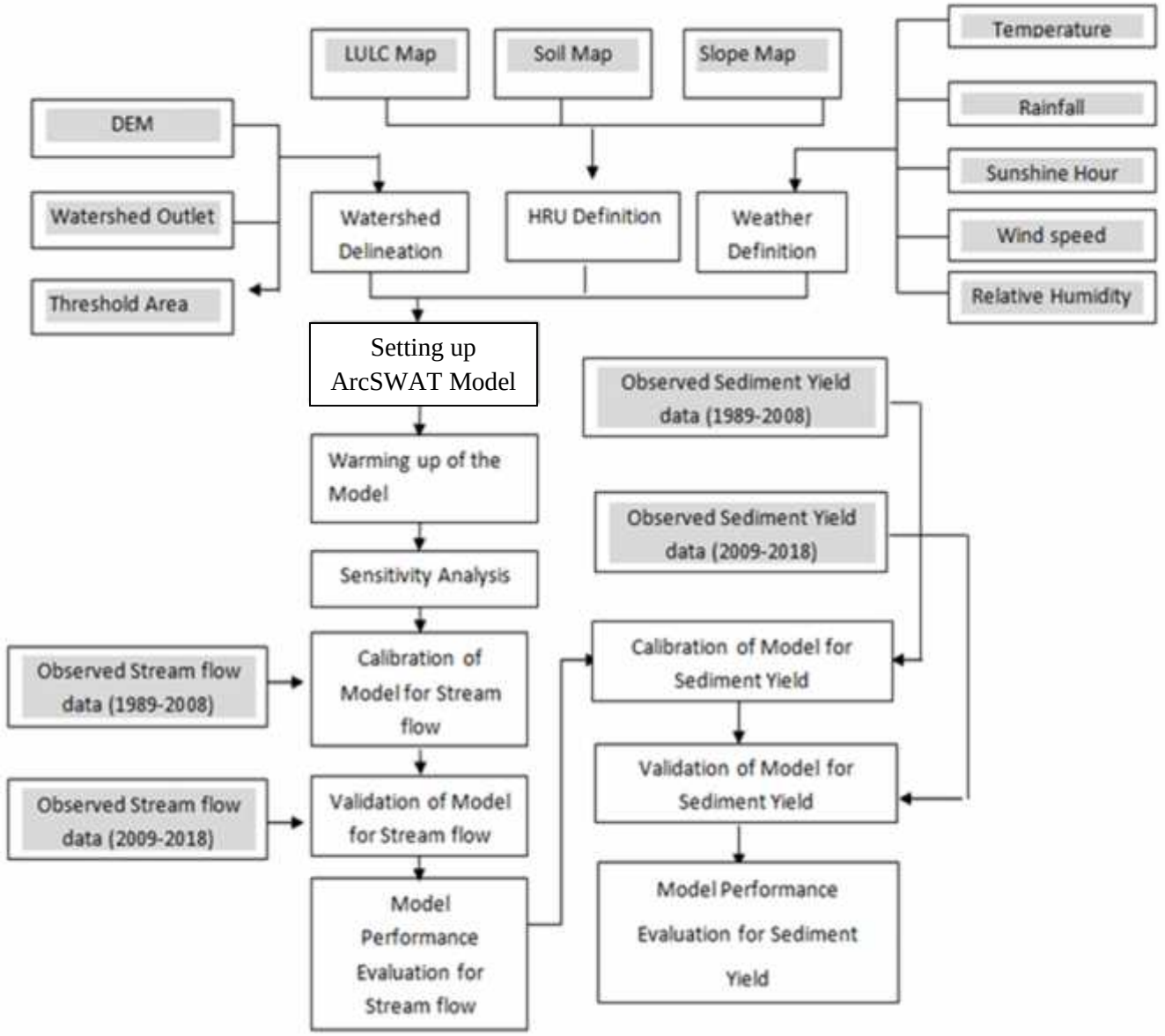

Figure 3. 8: Conceptual framework of the study

CHAPTER FOUR

RESULTS AND DISCUSSION

4.1 Land use land cover change

4.1.1. Land use land cover classification and Accuracy assessment

In this study, supervised classification methods have been applied on ERDAS IMAGINE software and the land use land cover maps were prepared based on the training data statistics (Table 3.2). There are six land use land cover classes in this study such as agricultural land, shrub land, forest, bare land, built-up and water body. The classification of satellite imagery for the four study periods provided the spatial distribution of land use land cover categories. Figure 4.1 and 4.2 shows the land use and land cover maps of 1989, 1999, 2009 and 2018 which have undergone significant land use land cover change for the specified period.

To assess the classification accuracy, confusion matrix had been used including overall accuracy, user's accuracy, and producer's accuracy. Classification is not complete until its accuracy is assessed using the known Kappa statistics.

Accordingly to the analysis the overall accuracy results of the classified images were 87.22 %, 90.56%, 91.67% and 89.44%, respectively for the years 1989, 1999, 2009 and 2018. According to Geremewu (2013) the minimum accuracy value for reliable land cover classification is 85 %. On the other hand, based on the result the overall accuracy confirmed in the acceptable range. The resulting classification of land use land cover maps of the four periods had a Kappa statistics of 0.82, 0.87, 0.89 and 0.84, for the periods 1989, 1999, 2009 and 2018, respectively. This was reasonably good in overall accuracy and accepted for the subsequent analysis and change detection (Lea and Curtis, 2010).

4.1.2. Land use land cover change detection

The land use and land cover change detection is carried out based on remote sensing images have been widely applied in research for land use and land cover change, natural resource management and environment monitoring & protection (Zhang et al., 2014).

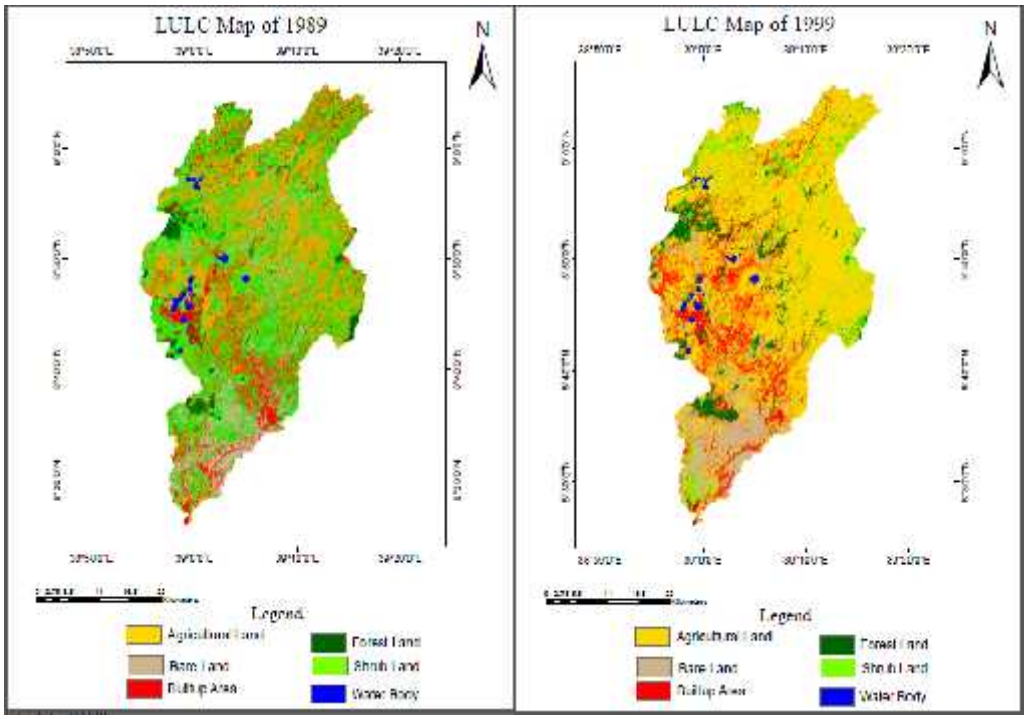

Figure 4. 1 Land use land cover map of A) 1989 and B) 1999, respectively

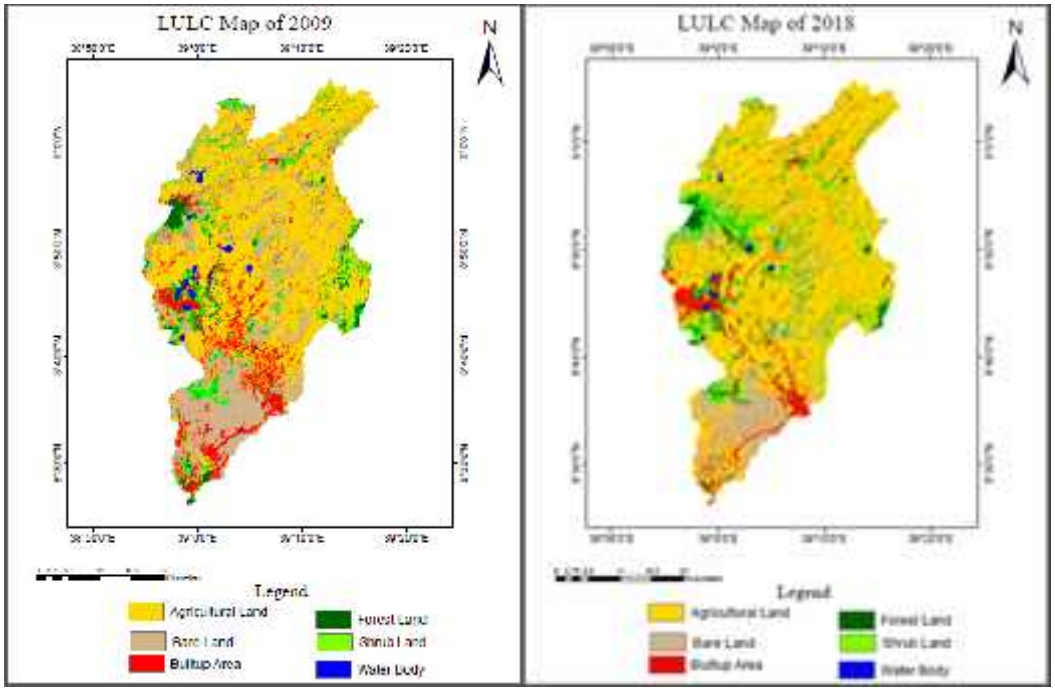

Figure 4. 2 Land use land cover map of A) 2009 and B) 2018, respectively

Land use land cover changes at Modjo watershed is summarized in Table 4.1. During the three decades (1989-1999, 199-2009 and 2009-2018) the land use land cover change has shown a similar trend. As it is presented in Figure 4.3 and Table 4.1 agriculture was the dominant land use (48.76%) followed by bare land (18.56%). Shrub land, forest, built-up and water body were the land use class having 15.10%, 7.00%, 9.32% and 1.26% share of the watershed respectively. These land use land cover types have common physical and geographical inter-connections, as an area increase in one type of land use category was associated with an area decrease in another land use category.

In the watershed more lands have experienced agricultural expansion due to the soil fertility and land suitability. Land under agriculture increased by 4.90% of total area due to the topographic suitability of the area and the increase of population growth that causes the increase in demand of cultivation land for different agricultural production.

Table 4. 1 Land use and land covers and change detection

Land use and land cover type	**Land use and land covers**							
	1989		**1999**		**2009**		**2018**	
	Area(ha)	**%**	**Area(ha)**	**%**	**Area(ha)**	**%**	**Area(ha)**	**%**
Water Body	2141.93	1.26	2002	1.18	1844.24	1.08	1773.65	1.04
Bare land	31600.9	18.56	20117.6	11.82	19631.5	11.53	12751.8	7.49
Built-up	15865.9	9.32	19577.3	11.50	21167.5	12.43	28693	16.85
Forest	11926.3	7.00	11294.3	6.63	9645.08	5.66	4427.5	2.60
Shrub	25705.9	15.10	20362.8	11.96	14523.11	8.53	13511.48	7.94
Agriculture	83025.5	48.76	96911.9	56.92	103455	60.76	109109	64.08
Total	170266.4	100.00	170266.4	100.00	170266.4	100.00	170266.4	100.00

Table 4. 2 Land use and land cover change during the periods 1989-1999, 1999-2009, 2009-2018 and 1989-2018

Land use and land cover type	Land use and land cover change							
	1989-1999		1999-2009		2009-2018		1989-2018	
	Area(ha)	%	Area(ha)	%	Area(ha)	%	Area(ha)	%
Water Body	-139.93	-0.082183	-157.76	-0.009	-70.59	-0.0041	-368.28	-0.22
Bare land	-11483.3	-6.744314	-486.1	-0.029	-6879.7	-0.4041	-18849.1	-11.07
Built-up	3711.4	2.179761	3711.4	0.218	7525.5	0.44198	12827.1	7.53
Forest	-632	-0.371183	-632	-0.037	-5217.58	-0.3064	-7498.8	-4.40
Shrub	-5343.1	-3.138082	-5343.1	-0.314	-1011.63	-0.0594	-12194.4	-7.16
Agriculture	13886.4	8.15569	13886.4	0.8156	5654	0.33207	26083.5	15.32

Note: Negative and positive signs indicate the decrease and increase of LULC class, respectively.

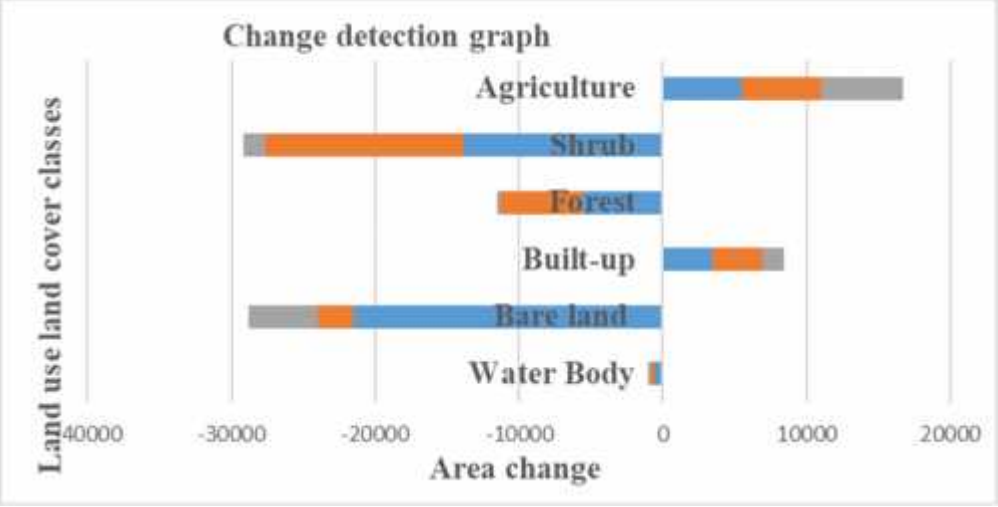

Figure 4. 3 Chart for land use land cover change detection

Research results of the previous studies indicate the same trend. For instance, (Rientjes et al., 2011) also evaluated the land cover change impact in the Upper Gilgel Abbay catchment of the Upper Blue Nile basin. There is a significant decrease in forest cover mainly due to expansion of agricultural land. According to Hadgu et al. (2008) identified that there was decrease of natural vegetation and expansion of agricultural land over a period of 41 years in Tigray, northern part of Ethiopia. Figure 4.3 above clearly shows that percentage of cover of the land use and land covers and patterns of the changes took place during the study periods due to adverse impact of climate in the study area.

During the second decade (1999-2009), percentage increase of agricultural land by 1386.4 ha and increase of built-up by 3711.4 ha. A decrease of water body 157.76 ha, bare land by 486.1 ha, forest by 632 ha and shrub land by 5343.1 ha, respectively due to expansion of agriculture and increase of built-up area. The same increasing trend of agriculture and built-up was observed in period 2009-2018, and on the other hand there has been a decreasing trend on bare land, shrub, forest and water body. The driving forces behind these changes were economic development, agricultural expansion and population growth. Water decrease is occurred due to the gradual conversion of water area into agricultural land during the three decades.

In this study, there is significant expansion of built-up and agricultural were noticed. According to the result of Table 4.2, agricultural land was increased by 26,083.5 ha and this shows agriculture was the dominant land use land cover change type in the area. Built-up area was showed an increase of 12,827.1 ha during the study period 1989-2018 next to agriculture. On the other hand there is a decrease of water body, bare land, forest and shrub by 368.28 ha, 188, 44 9.1 ha, 7,498.8 ha and 12,194.4 ha, respectively.

4.2. Streamflow modeling

4.2.1. Streamflow sensitivity analysis

The sensitivity analysis was based on results from the first simulations. As initial settings, streamflow data from Modjo gauge station were used and the analysis was carried out using a built-in SWAT sensitivity analysis tool. As a result, 16 sensitive parameters were identified which have association with hydrological processes, and mostly related to surface runoff and base flow. Based on the results obtained from sensitivity analysis using SUFI-2, the ranks of parameters assigned depending on p-value and t-stat. P-value indicates significance of sensitivity and t- stat provides the measure of parameter sensitivity (Abbaspour, 2014). Larger in the absolute value of t-stat means the parameter is more sensitive and p-value closer to zero means parameter has more significance.

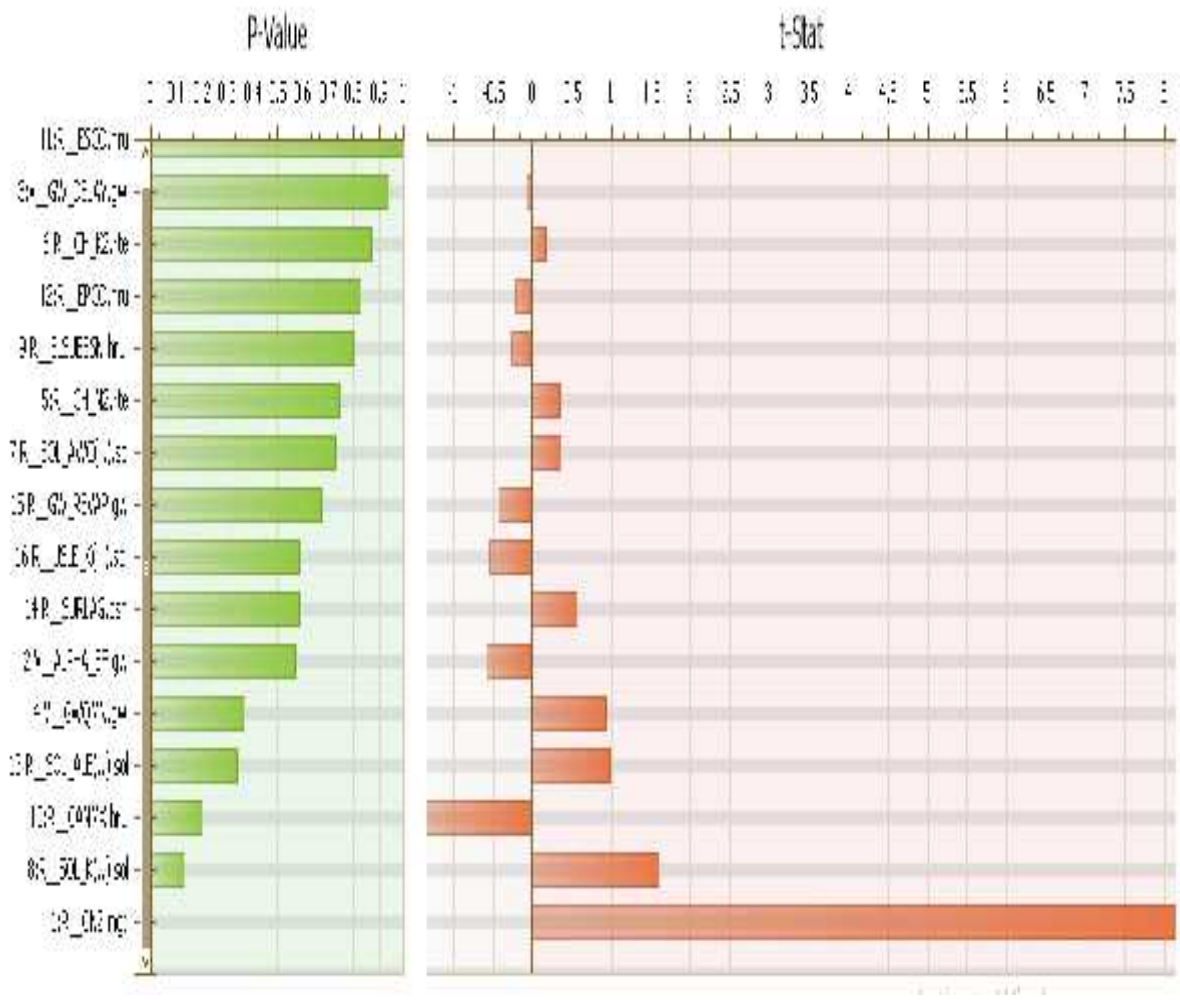

Figure 4. 4 p-value and t-stat for sensitivity analysis of streamflow

During sensitivity analysis for stream flow SCS runoff curve number (CN2) has the lowest p-value and highest t-stat, and it indicate that SOL-AWC was the most sensitive parameter of the watershed. Available water capacity of the soil layer (SOL AWC) is a parameter which is highly sensitive next to SCS runoff curve number (CN2) during streamflow calibration. On the other hand Soil evaporation compensation factor (ESCO) and Groundwater delay (days) (GW-DELAY) have highest p-value and lowest-stat, and this indicate that ESCO is the least sensitive parameter for streamflow.

Table 4. 3 sensitive parameters selected for streamflow calibration and validation

No	Parameter name	Description of parameters	t-stat	P-value	Value range	Rank
1	CN2	SCS runoff curve number	8.14	0.00	35-98	1
2	SOL-K	Saturated hydraulic conductivity	1.59	0.13	0-2000	2
3	CANMAX	Maximum canopy storage	-1.34	0.2	0-100	3
4	SOL-ALB	Moist soil albedo	1.26	0.34	0-0.25	4
5	GWQMN	Threshold depth of water in the shallow aquifer required for return flow to occur	0.93	0.36	0-5000	5
6	ALPHA-BF	Base flow alpha factor	-0.57	0.57	0-1	6
7	SURLAG	Surface runoff lag time	0.56	0.58	0.05-24	7
8	USLE-K	USLE equation soil erodibility (K) factor	-0.55	0.59	0-2000	8
9	GW-REVAP	Groundwater "revap" coefficient	-0.42	0.67	0.02-0.2	9
10	SOL-AWC	Available water capacity of the soil layer	0.35	0.72	0-1	10
11	CH-N2	Manning's "n" value for the main channel	0.33	0.74	0.01-0.3	11
12	SLSUBBSN	Average slope length	-0.25	0.79	10-150	12
13	EPCO	Plant uptake compensation factor	-0.21	0.83	0-1	13
14	CH-K2	Effective hydraulic conductivity in main channel alluvium	0.16	0.87	0.01	14
15	GW-DELAY	Groundwater delay (days)	-0.07	0.94	0-500	15
16	ESCO	Soil evaporation compensation factor	-0.00	0.99	0-1	16

4.2.2. Streamflow calibration and validation

Model warm-up period comprises the first two years of data series (1988-1990). Streamflow calibration and validation periods were between 1990 to 2008 and 2009 to 2018 for Modjo gauging station respectively. The sediment generated from each HRU and sub basin is primarily governed by soil, hydrologic and hydraulic parameters such as soil erodibility, surface runoff, stream discharge and stream flow velocity. Therefore, prior to sediment calibration, stream flow should be calibrated and discussions are presented in the following sub-sections.

Stream flow data at Modjo gauging station was used to calibrate the SWAT model for the years 1989-2008. Model calibration was carried out on monthly bases through fine adjustments on identified basic parameters. During the calibration period from 1990-2008, the simulated average monthly flow matched well with the average monthly measured flow (with R^2 = 0.76, NSE = 0.57 and PBIA= -21.3). Uncertainty measure values during the calibration period are P-factor=0.46 and R-factor=0.68.

The comparison between the simulated versus observed average monthly flow was shown in Figure 4.7. The simulated flow data closely matched the observed flow over the entire period. As it can be witness from the monthly observed and simulated flow the watershed gets highest amount of flow on the months of June, July and August. Simulated values are over predicted than observed values except few observed months which predicts more than simulated. Detailed report was described in Table 4.5 for flow in Modjo watershed. The SWAT model simulation results fall under a good category according to the performance criterion of (Moriasi et al., 2007).

SWAT model was successfully validated for stream flow from 2009 to 2018. Monthly flow rates were well predicted and measured, and simulated monthly flow matched well based on the simulated results of R^2= 0.78, NSE = 0.69, RSR=0.56, PBIAS= -16.6, P-factor= 0.19 and R-factor=0.00. Averaged monthly Stream flow simulation during validation period behaves similarly with that of calibration period. As shown in the Figure 4.6, the model under estimated observed flow than simulated flow except for few periods which over estimates observed flow during validation.

Uncertainty measure of SUFI-2 showed that P-factor of 0.46 and R-factor of 0.68 for calibration and P-factor of 0.19 and R-factor of 0.00 for stream flow validation. It is clearly indicated that about 75% of data for the calibration and 78% of data for the validation was bracketed by the 95PPU band with a better strength of estimation (R-factor <1) for both cases.

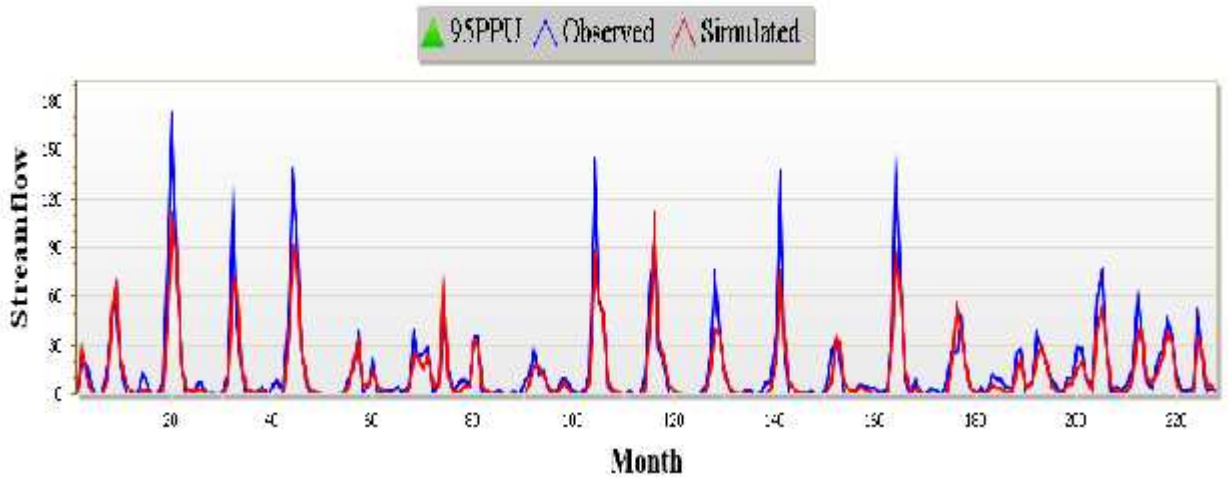

Figure 4. 5 Simulated vs observed average monthly flows generated from SWAT CUP during calibration

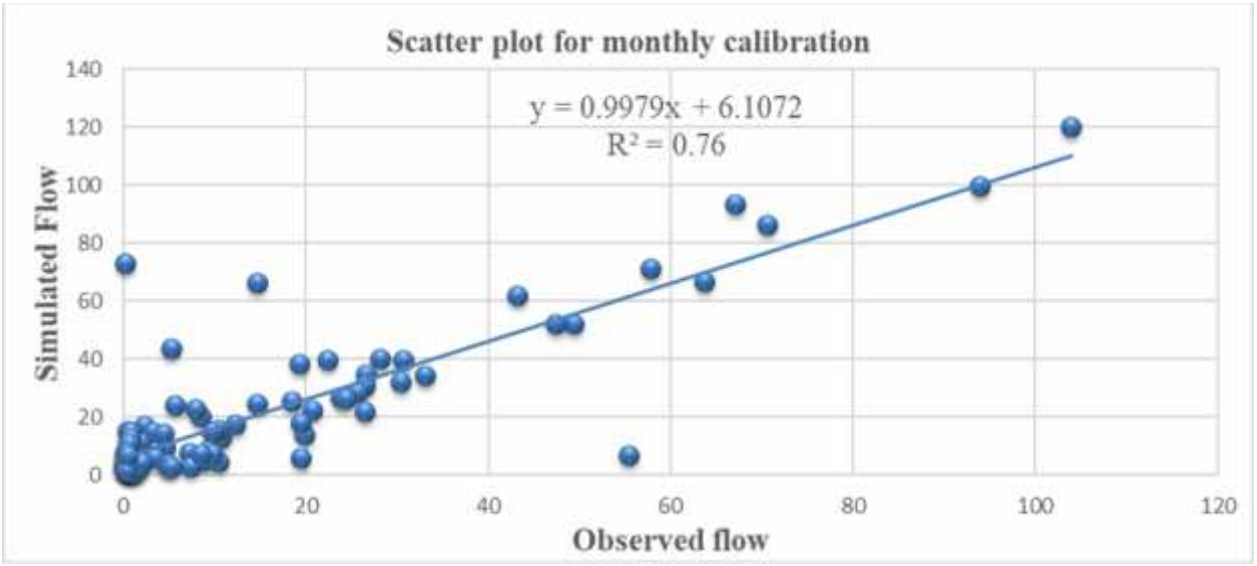

Figure 4. 6 scatter plot of the simulated vs observed average monthly flow during calibration

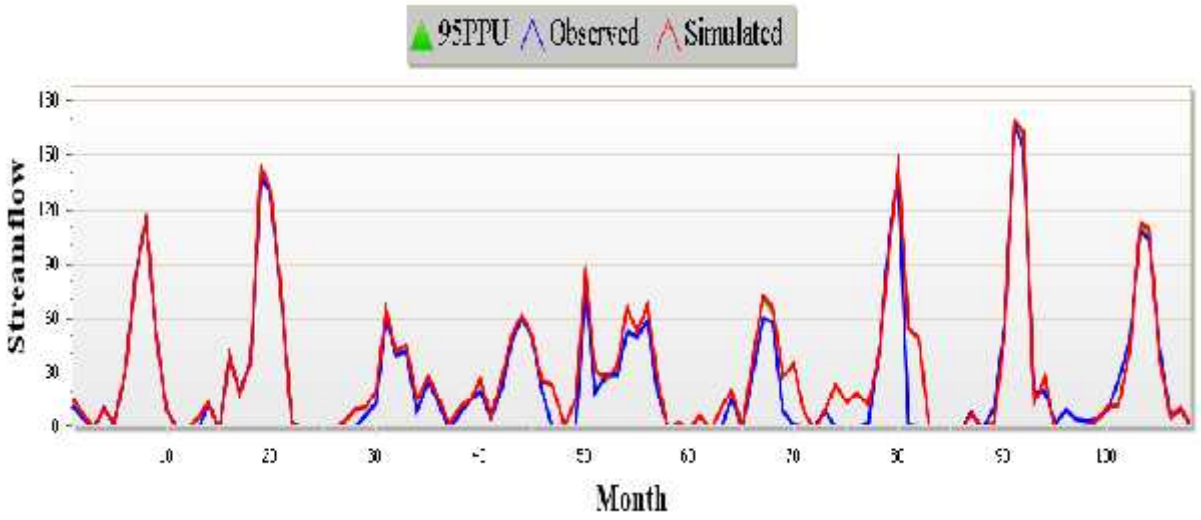

Figure 4. 7 simulated vs observed average monthly flows generated from SWAT CUP during validation

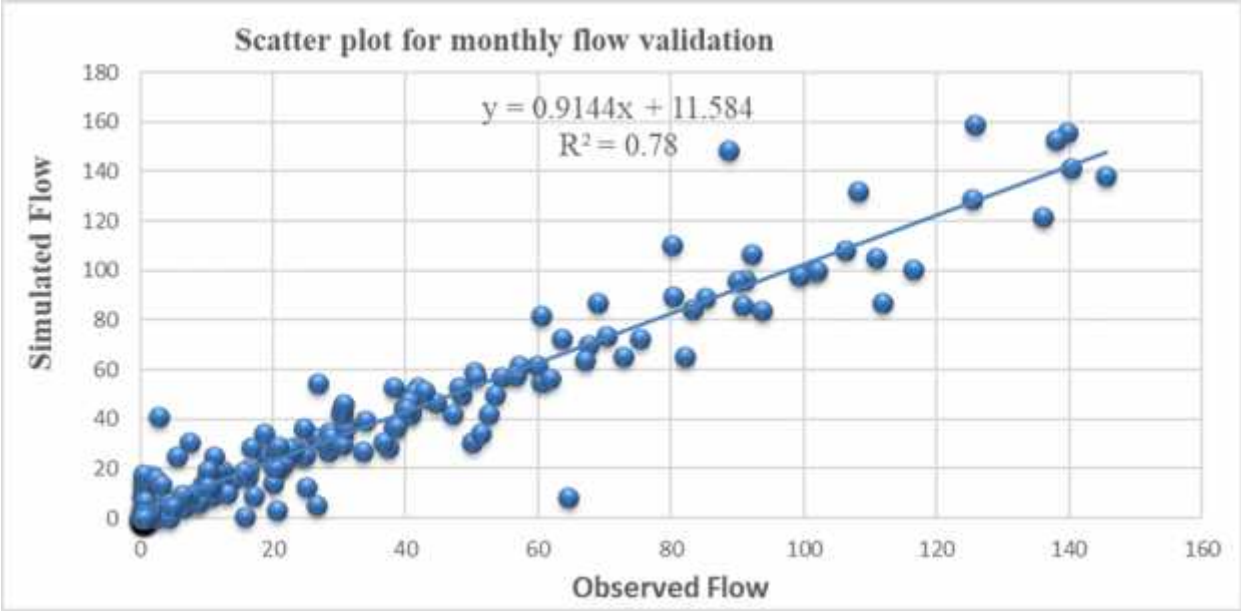

Figure 4. 8 scatter plot of the simulated vs observed average monthly flow during validation

During the calibration and validation periods, the difference between the simulated and observed values might be attributed to the inadequate representation of rainfall inputs, due to uneven distribution of rain gauge stations in the catchment; the spatial variability of rainfall; errors during data recording; or local rainfall storms that were not well represented by the rainfall data used in the hydrological simulations.

The scatter plots of observed and simulated daily stream flow for the calibration and validation periods along with the 1:1 and regression lines are shown in Figure 4.6 and 4.8 respectively. It is observed from Figure. 4.5 There is more under prediction of higher streamflow values, low stream flow values are evenly and closely scattered around the 1:1 line. For streamflow validation, low stream flow values are scattered near the 1:1 line, but most of the higher streamflow values are over predicted Figure 4.7 with the exception of two very high streamflow which are under predicted.

Table 4. 4 Summary of model performance measures for monthly streamflow at Modjo watershed (1989- 2018)

Simulation	**Model performance indicators**				**Uncertainty measures**	
period	**R^2**	**NSCE**	**RSR**	**PBIAS**	**P-factor**	**R-factor**
Calibration (1990-2008)	0.76	0.57	0.66	-21.3	0.46	0.68
Validation (2009-2018)	0.78	0.69	0.56	-16.6	0.19	0.00

The result shown in Table 4.4 indicates very close to the result obtained by (Golmohammadi et al., 2014) from the analysis of SWAT for continuous hydrologic simulations. They obtained NSE, R^2, and RSR values of 0.73, 0.64, and 0.34, respectively, for monthly time intervals.

4.3. Sediment yield modeling

4.3.1. Sediment yield Sensitivity Analysis

During sensitivity analysis of sediment yield twelve sediment parameters were checked using SUFI-2 in SWAT-CUP. Based on the results obtained from sensitivity analysis, ranks of sediment parameters were assigned depending on p-value and t-stat (Figure 4.9).

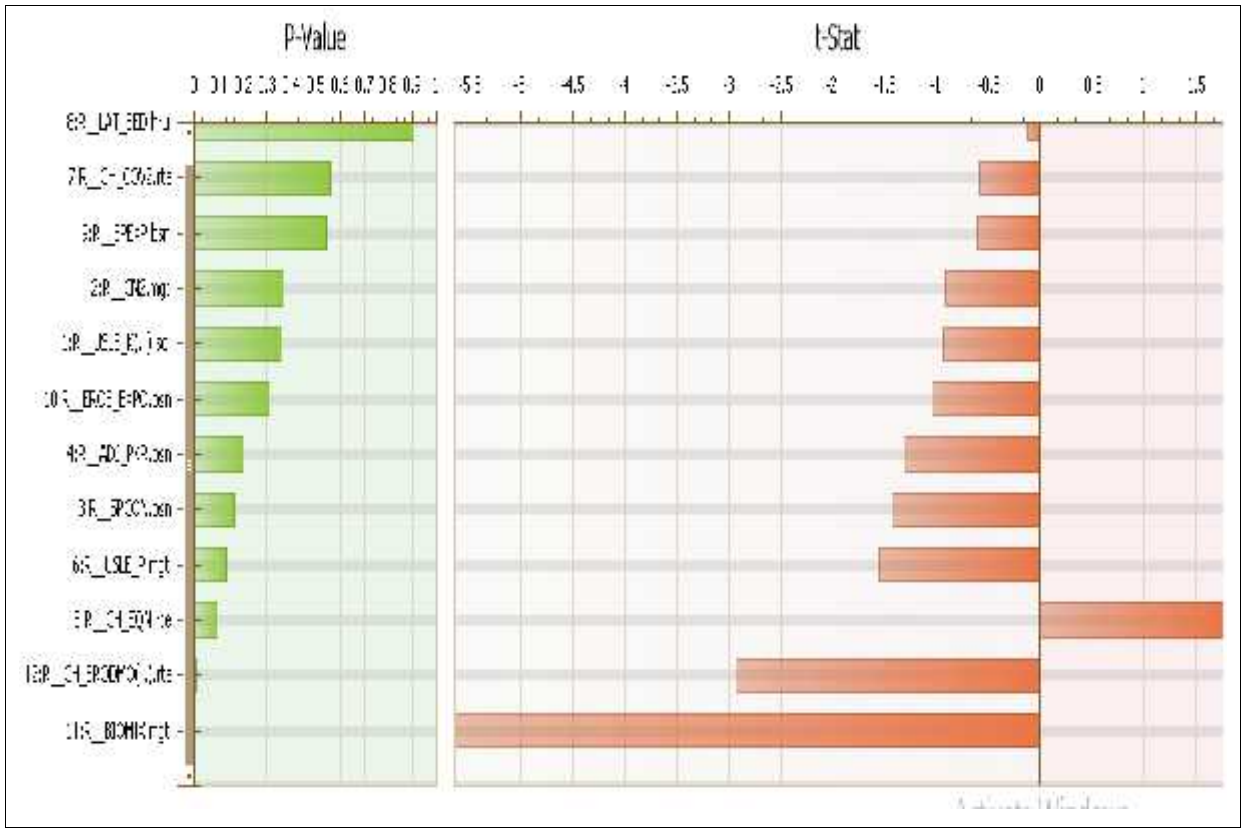

Figure 4. 9 p-value and t-stat for sensitivity analysis of sediment yield

The first three most sensitive parameters for sediment yield calibration were Biological mixing efficiency (BIOMIX), channel erodibility factor (CH-ERODMO) and Sediment routing method (CH-EQN). These parameters have lowest p-value and highest t-stat. The rest ranked sensitive parameters for sediment yield are presented in Figure 4.7 Sediment concentration in lateral flow and groundwater flow (LAT-SED) has highest p-value and lowest t-stat. From the analysis it is evident that LAT-SED is the least sensitive parameter in relation to sediment yield calibration and validation for the catchment.

Table 4. 5: sensitive parameters selected for sediment yield calibration and validation

No	Parameter name	Description of parameters	t-stat	P-value	Value range	Rank
1	BIOMIX	Biological mixing efficiency	-5.65	0.0005	0-1	1
2	CH-ERODMO	channel erodibility factor	-2.93	0.00683	0-1	2
3	CH-EQN	Sediment routing method	1.75	0.09	0-4	3
4	USLE-P	USLE equation support practice factor	-1.55	0.13	0-1	4
5	SPCON	Linear parameter calculating the (max) sediment	-1.43	0.16	0.0001-1	5
6	ADJ-PKR	Peak rate adjustment factor for sediment rout	-1.30	0.20	0.5-2	6
7	EROS-EXPO	An exponent in the overland flow erosion equation	-1.04	0.30	1.5-3	7
8	USLE-K	USLE equation soil erodibility (K) factor	-0.93	0.35	0-2000	8
9	CN2	SCS runoff curve number Channel cover factor	-0.91	0.36	35-98	9
10	SPEXP	Exponent parameter for calculating sediment	-0.60	0.54	1-1.5	10
11	CH-COV_2	Channel erodibility factor	-0.58	0.56	0.001-1	11
12	LAT-SED	Sediment concentration in lateral flow and groundwater flow	-0.12	0.904	0-5000	12

4.3.2. Sediment yield Calibration and Validation

Stream flow was obtained by converting a continuous water level (m) records (using pressure transducer) into flow (m^3/s) based on an experimentally developed water level and discharge rating curve according to (Zehetbauer et al., 2013).

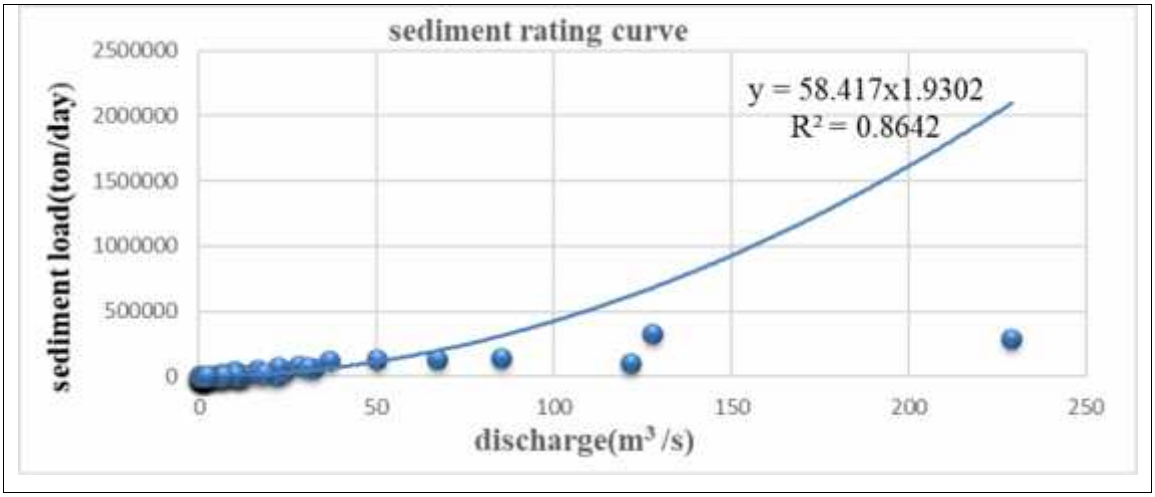

Figure 4. 10 Sediment rating curve of Modjo watershed

A continuous daily time step sediment yield for the Modjo station was generated by using the sediment rating curve equation (Equation 3.8 and 3.9)

SWAT model using the calibration period from 1990- 2008, the agreement between observed and predicted sediment yield was indicated by (with R^2 = 0.71, NSE = 0.71 and PBIA= 8.0). Uncertainty measure values during the calibration period were found as P-factor=0.96 and R-factor=0.01 which indicated that about 96% of the sediment data could be bracketed by the 95PPU band with a better strength of estimation 0.01 which is close to a perfect 0 for both calibration and validation.

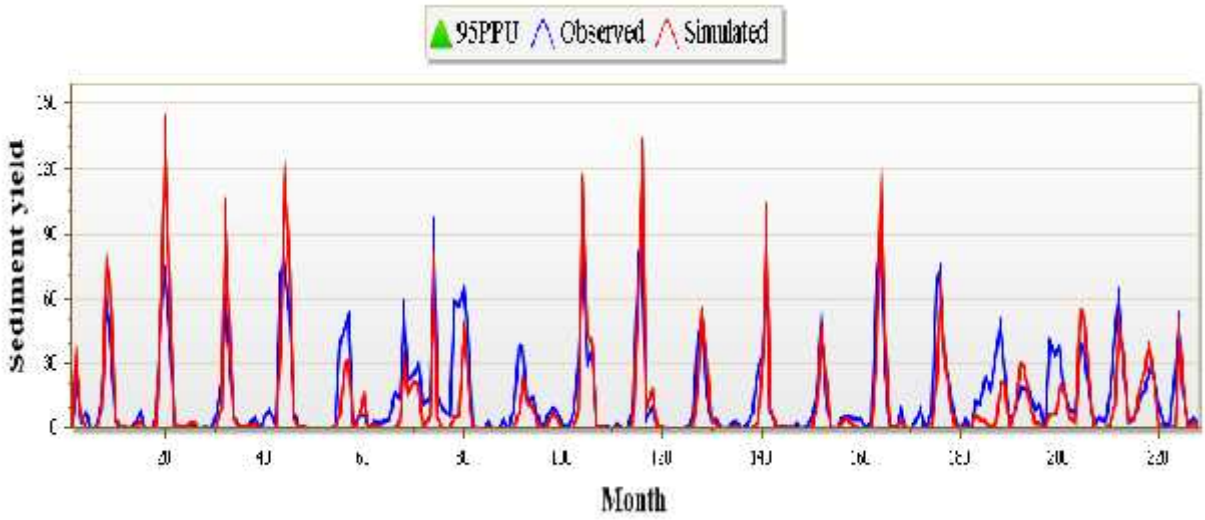

Figure 4. 11 Simulated vs observed average monthly sediment yield generated from SWAT CUP during calibration

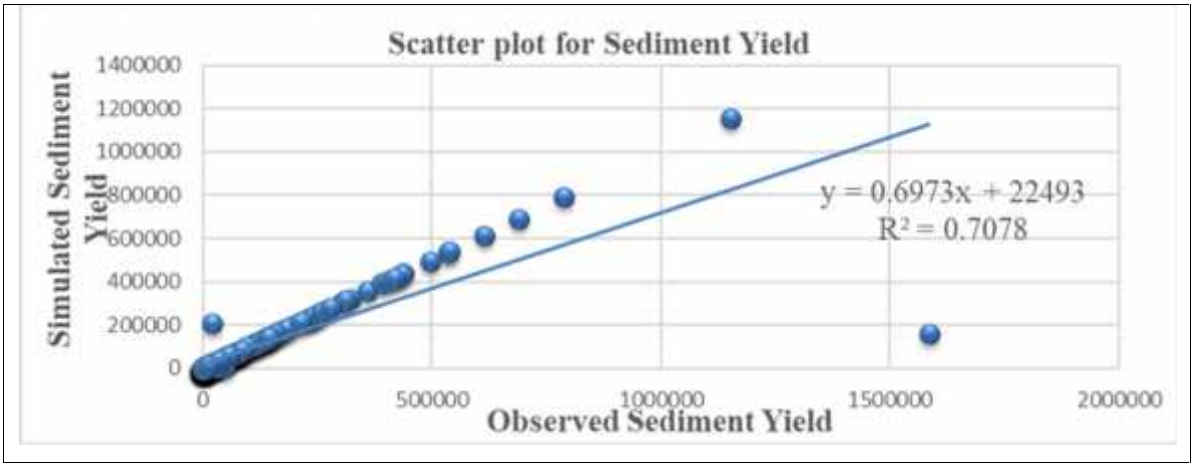

Figure 4. 12 scatter plot of the simulated vs observed sediment yield during calibration

According to model performance evaluation criteria listed under (Appendix Table 1) the sediment simulation result for calibration and validation at Modjo watershed showed a very good performance with R^2= 0.71, NSE of 0.76, RSR of 0.54 and PBIAS of 8.0% for calibration and R^2 of 0.86, NSE of 0.78, RSR of 0.47 and PBIAS of -20.2% for validation.

Moriasi et al. (2007) proposed that NSE values should exceed 0.5 in order for model results to be judged satisfactory for hydrologic evaluations performed on a monthly time step.

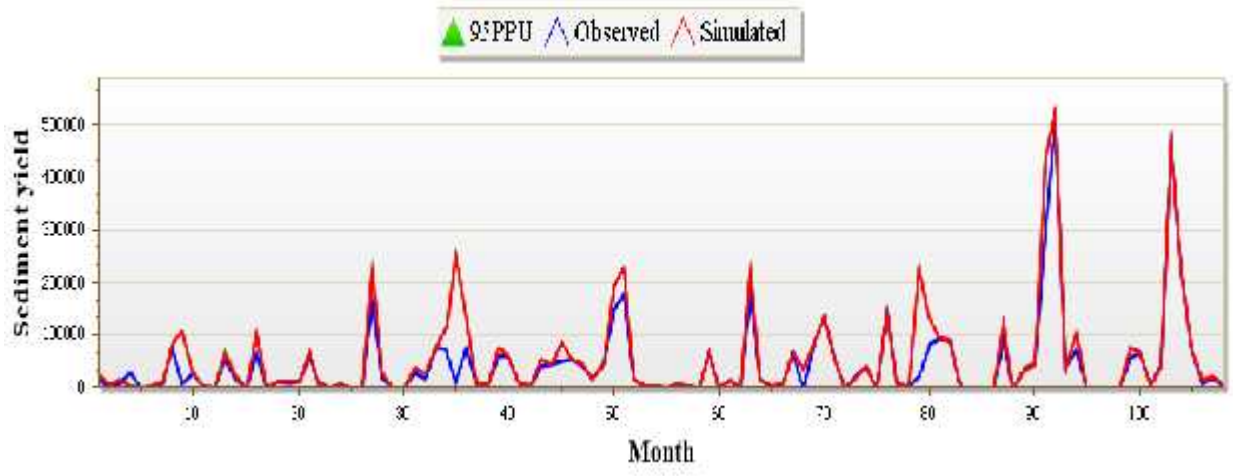

Figure 4. 13 Simulated vs observed average monthly sediment yield generated from SWAT CUP during validation

Sediment yield graphs shown in (Figure 4.12 and 4.14) indicate that the model slightly overestimated sediment yield from the watershed in most of the year and underestimated in some years. This is the same discussion with the flow hydrograph discussed in streamflow section due to the sediment yield is directly proportional to generated erosion and flow in the river.

Uncertainty measures of SUFI-2 showed that P-factor of 0.96 and R-factor of 0.01(close to a perfect 0) for calibration, and P-factor of 0.64 and R-factor of 0.01 for validation are also acceptable for SWAT-CUP model sediment predictions. This indicated that about 96% (Out of a perfect 100 %) of the sediment data could be bracketed by the 95PPU band with a better strength of estimation 0.04 which is close to a perfect 0 for both calibration and validation.

Scatter plots of sediment yield shown in Figure 4.12 and 4.14 shows a high correlation between observed and simulated data on 1:1 regression line for calibration and validation periods.

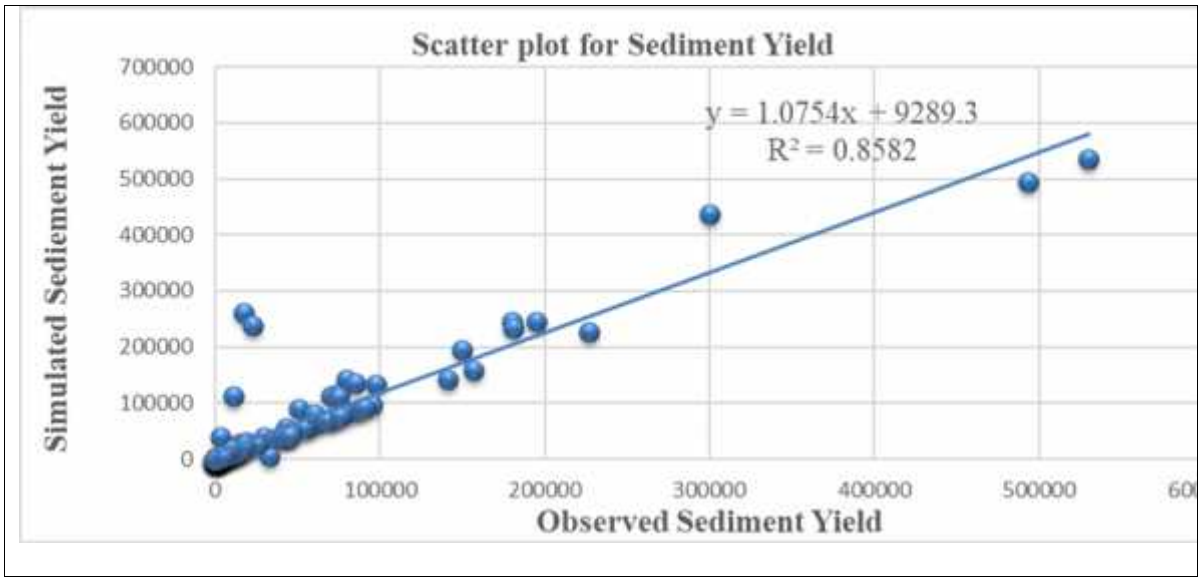

Figure 4. 14 scatter plot of the simulated vs observed sediment yield during validation

Table 4. 6: Summary of model performance measures for monthly sediment yield at Modjo water-shed (1989- 2018)

Simulation	**Model performance indicators**				**uncertainty measures**	
period	**R^2**	**NSE**	**RSR**	**PBIAS**	**P-factor**	**R-factor**
Calibration (1990-2008)	0.71	0.71	0.54	8.0	0.96	0.01
Validation (2009-2018)	0.86	0.78	0.47	-20.2	0.64	0.01

4.4. Impact of Land use land cover change on streamflow and sediment yield

4.4.1. Impact of Land use land cover change on streamflow

The SWAT model estimated important water balance components in addition to the annual and monthly flow. The most important elements of water balance of a basin are precipitation, surface runoff, lateral flow, base flow, and evapotranspiration. Among these, all the variables, except precipitation, need prediction for quantifying due to their difficulty on measurement.

Annual water balance components of Modjo watershed were simulated by SWAT model using principle of conservation of mass (Equation 2.1). Simulated annual water balance components showed that average annual precipitation falling on basin was 931.93mm and evaporation loss from the basin was 549.82mm which accounts 54.73% from annual water budget. Surface runoff (SURF Q), lateral flow (LAT Q) and ground water flow (GW Q) results were 208.6mm (12.25%), 1.21mm (0.071%) and 195.2mm (11.4%), respectively. Megersa et al. (2017), reported that the simulated average annual sediment yield and surface runoff were 105.243 t/ha and 366.14 mm respectively for the conversion of land use to agriculture whereas the simulated average annual sediment yield and surface runoff were 66.88 t/ha and 271.23 mm respectively for base scenario.

Total water yield, which is the amount of stream flow leaving the outlet of watershed on monthly time step in combination with surface runoff, lateral and ground water accounts 416.12mm (24.44%) from annual water budget. Average annual water yield of Modjo watershed for the analysis period 1990-2018 was 416.13mm by using land use land cover map 1989 which is baseline period for this particular study. Average annual sediment loading of the watershed was 13.93 t/ha/yr. These results are consistent with previous study by (Lewoye, 2021) on Anjeb watershed; Northern Ethiopia reported the average annual sediment yield of 22.5 t/ha/ yr.

As it is shown in the Table 4.7 the watershed gets maximum precipitation on the months of June (102.76mm), July (227.41mm) and August (226.66mm). Maximum sediment yield was observed on the months of July (4.13 t/ha) and Aug (4.4 t/ha), and water yield of 102.37 m^3/s in average monthly time step.

Table 4. 7: Average monthly basin values

Month	PCP (mm)	SURF-Q(mm)	LAT-Q(mm)	Water Yield(mm)	ET(mm)	Sediment Yield(t/ha)	PET(mm)
1	18.76	3.63	0.04	8.86	23.93	0.3	62.8
2	33.68	8.01	0.03	11.59	54.31	0.57	85.25
3	50.93	7.14	0.04	11.22	84.03	0.64	139.19
4	55.61	6	0.04	9.09	63.03	0.65	116.26
5	57.42	6.92	0.05	9.04	53.47	0.64	105.1
6	102.76	14.79	0.06	16.89	51.46	1.24	88.86
7	227.41	56.64	0.15	62.78	73.95	4.13	100.15
8	226.66	69.48	0.27	102.37	21.59	4.4	26.31
9	102.97	25.5	0.25	84.95	45.72	0.51	69.46
10	27.78	5.83	0.15	54.98	44.09	0.52	99.37
11	14.72	2.13	0.08	28.67	29.85	0.14	87.56
12	12.93	2.47	0.05	15.6	3.93	0.19	9.85
Total	931.93	208.54	1.21	416.13	549.36	13.93	990.16

PCP=Precipitation, SURF Q=Surface flow, LAT Q= Lateral flow, ET=Actual Evapotranspiration and PET= Potential Evapotranspiration.

In the observed period (1989–2018) on Table 4.7, there is no increasing trend in annual precipitation according to the records from four meteorological stations (Chefe Donsa, Debrezeyit, Ejere and Modjo). Water balance results for different land use land cover periods described in Table 4.4 shows visible variations, that is increasing trend in all water balance components (SURF-Q, LAT-Q, WATER YIELD and PET) except evapotranspiration, which indicates decreasing trend in annual time step. This is because of the expansion of agricultural land over forest that results in the increase of surface runoff following rainfall events.

Table 4. 8 Average annual basin values for land use land cover maps

LULC Map	PCP(mm)	SURF-Q(mm)	LAT-Q(mm)	WATER YIELD(mm)	ET(mm)	PET(mm)
1989	931.6	208.54	1.21	416.04	549.36	990.16
1999	931.9	256.21	11.09	443.01	506.9	999.5
2009	931.9	278.99	11.87	473.49	443.2	905.2
2018	931.9	306.31	14.35	487.87	472.2	903.1

4.4.2. Impact of Land use land cover change on sediment yield

The total observed and simulated sediment yield (load) from Modjo watershed presented on Figure 4.16 during the period from 1990 to 2018 was 104,988 ton/year and 97,690 ton/year, respectively. About 54.75% of total watershed area identified as sediment prone areas. According to the report Melka (2010) on sediment yield modeling using SWAT, Case study of Upper Awash Basin Ethiopia, total sediment load in ton/year during a period from 1997-2003 was 110458.4 ton/ha and 108539.6 ton/ha for both observed and simulated sediment on Modjo watershed.

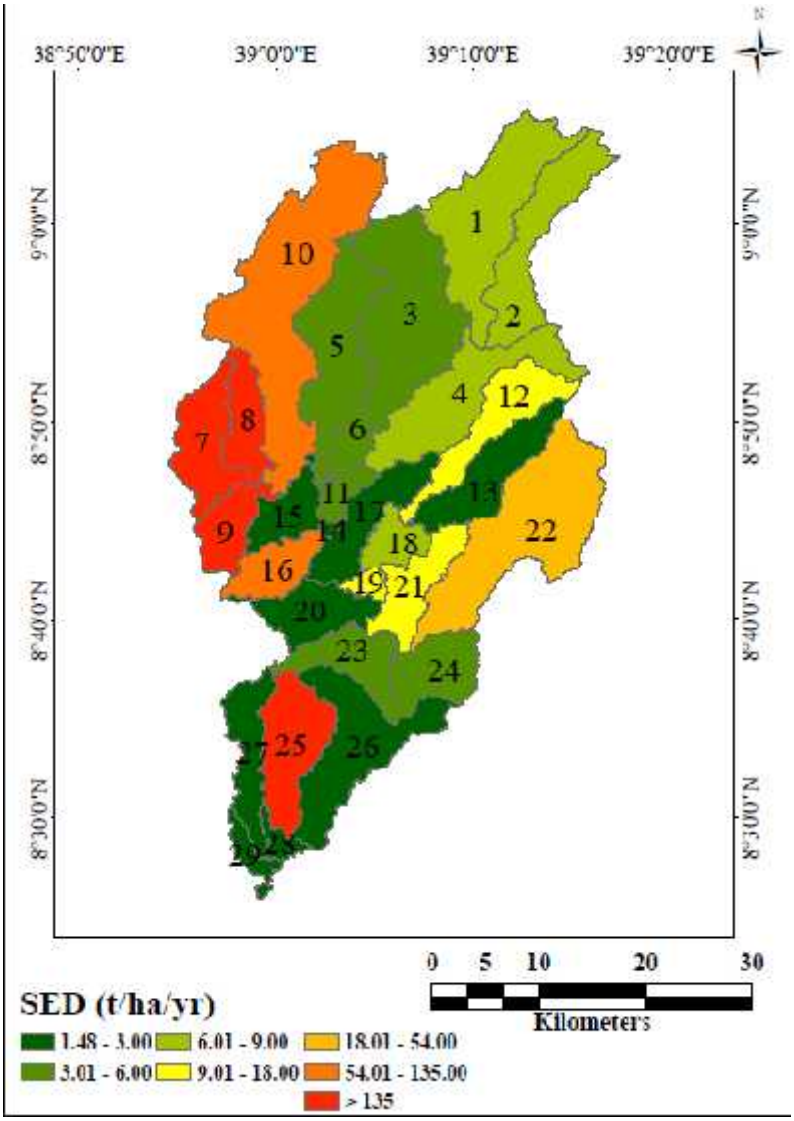

Figure 4. 15 Spatial distribution of sediment yield

The above figure (Figure 4.15) indicates spatial distribution of sediment yield of Modjo watershed under sub basin level for the baseline scenario. According to the figure report, sub basin 8 had contributed 446.88 t/ha/yr and it is highest amount of sediment yield generated during the time from that particular sub basin. Sub basin 7, 9 and 25 contributed 377.17, 305.72 and 258.37t/ha/yr, respectively. Sub-basin 15 contributed 1.48 t/ha/yr and it is the minimum amount of annual sediment yield from Modjo watershed.

Figure 4. 16 Observed and simulated sediment yield of Modjo watershed

CHAPTER FIVE

CONCLUSIONS AND RECOMMENDATIONS

5.1. Conclusions

Land use land cover changes have a significant impact on stream flow and sediment yield on the Modjo watershed. Nowadays, hydrological models are highly applicable in the in fields of water resources management. The aim of modeling and data availability are the necessary criteria for selecting hydrological models. For this particular study SWAT hydrological model was selected to analyze land use land cover dynamics on stream flow and sediment yield.

Land use land cover classification by using ERDAS IMAGINE software was the primary activity which was done during the analysis after down loading four Land sat satellite images for the periods of 1989, 1999, 2009 and 2018. The overall accuracy results of the classified images were 87.22 %, 90.56%, 91.67% and 89.44%, respectively .Change detection for the four land use land cover maps were done. During the study period, agricultural expansion and built-up area showed an increase by 26,083.5 ha and 12,827.1 ha, respectively which showed that agriculture was the dominant land use land cover type on the area. On the other hand there is a decrease of water body, bare land, forest and shrub by 368.28 ha, 188,449.1 ha, 7,498.8 ha and 12,194.4 ha, respectively due to economic development, agricultural expansion and population growth.

The performance of the model was evaluated by different statistical indices and found as R^2=0.76, NSE=0.57, PBIAS= -21.3, P-factor=0.46 and R-factor=0.68 for streamflow calibration; R^2=0.78, NSE=0.69, PBIAS=16.6, P-factor=0.19 and R-factor=0.00 for streamflow validation. Similarly, R^2=0.71, NSE=0.71, PBIAS=8.0, P-factor=0.96 and R-factor=0.01 for sediment yield calibration. R^2=0.86, NSE=0.78, PBIAS= -20.2, P-factor=0.64 and R-factor=0.01 for sediment yield validation. The finding confirmed that the SWAT model was capable of simulating stream flow and sediment yield for baseline period of Modjo watershed.

The average annual water yield of Modjo watershed is 416.13mm. Surface runoff (SURF-Q), lateral flow (LAT-Q) and ground water flow (GW-Q) were 208.6mm (12.25%), 1.21mm (0.071%) and 195.2mm (11.4%), respectively. Among the 29 sub-catchments, five (sub-catchments 8, 7, 9, 25, and 10) produced the highest sediment yield and are more exposed to erosion. The mean annual sediment yield of the watershed was 13.93 t/ha/yr and average annual sediment yield (load) from Modjo watershed during the period from 1990 to 2008 was 93228.6131 ton/year.

The average annual streamflow of Modjo watershed is 416.13mm and 487.87 mm in 1989 and 2018, respectively. Surface runoff (SURF- Q), lateral flow (LAT-Q) and ground water flow (GW-Q) were 208.6mm (12.25%), 1.21mm (0.071%) and 195.2mm (11.4%), respectively.

The mean annual sediment yield of the watershed was 13.93 t/ha/yr and 39.93t/ha/yr in the years 1989 and 2018, respectively. Among the 29 sub-catchments, five (sub-catchments 8, 7, 9, 25, and 10) produced the highest sediment yield and are more exposed to erosion. Average annual sediment yield (load) from Modjo watershed during the period from 1990 to 2008 was 93228.6131 ton/year.

5.1 Recommendations

Generally from this specific study the following recommendations drawn:

- This research was conducted focusing on the impact on land use land cover dynamics of streamflow and sediment yield. But the impact of climate change should also be taken under consideration for the future research.
- Appropriate management options for land use land cover dynamics has to be given an emphasis so as to reduce sedimentation problems, and water availability at watershed and basin level.
- Sediment reduction methods like terracing, contouring, grassed waterway and filter strip must be taken under consideration in order to reduce sedimentation problem on the watershed area.
- The Koka dam reservoir is one of the seriously affected reservoirs in the Awash River basin. This results deposition of sedimentation problem and a rapid decrease in the

reservoir storage capacity of Koka dam. In order to reduce the operational value and life span of the reservoir appropriate management and conservation practices are recommended to critical sediment source areas.

REFERENCES

Abbaspour. (2012). *SWAT-CUP SWAT Calibration and Uncertainty Programs.*

Agarwal C., Green, G. M., Grove, J. M., Evans, T. P., and Schweik, C. M., 2002. A Review and Assessment of Land-Use Change Models: Dynamics of Space, Time, and Human Choice. U.S. Department .

Arnold , J. G., Allen. P. M. and Bernhardt. G. (1995). SWAT - Soiland Water Assessment Tool. Draft Users Manual. USDA-ARS, and Temple, TX.

Arnold, J. G. (1993). A comprehensive surface- groundwater.

Aspinall, R. (2008). Basic and applied land use science. In R. Aspinal and M. Hill (Eds.), Land Use Change: Science, Policy and Management (pp. 3–15). New York: CRC Press.

Atasoy et al., M. B. (2006). Monitoring land use changes and determinating the suitability of land for different uses with digital Photogrammetry. Remote Sensing and Photogrammetry, Cairo, Egypt.

Ayivor and Gordon. (2012). Impact of Land Use on River Systems in Ghana. *West African Journal of Applied Ecology, 20*, 83-95.

Barros JX. (2004). Urban growth in Latin American cities: exploring urban dynamics through agent-based simulation. Doctoral Thesis, University of London, London.

Belay. (2002). Land use/cover changes in the Derekolli catchment of south Welo Zone of Amhara Region. *Eastern Africa Social Science Research Review, 18*.

Bergström, S. a. (1995). The HBV model. In: Sing, V.P. (Ed), Computer models of watershed hydrology. Water Resources Publications, Colorado, 443-476.

Bewket. (2003). Towards integrated watershed management in high land Ethiopia: the Chemoga watershed case study. *Open Access Library Journal, 44*.

Buishand, T. (1982). Some Methods for Testing the Homogeneity of Rainfall Records. *Journal of Hydrology, 58*, 11-27.

Chow, V. T. (1988). *Applied Hydrology.* United State of America: McGraw-Hill.

Cundrelik. (2003). Hydrological model selection for CFCAS project, Assessment of water resources risk and vulnerability to change in climate condition, University of Western Ontario.

DeFries R, Eshleman KN (2004). Land-use change and hydrologic processes: a major focus for the future. Wiley InterScience, Hydrol, 18, 2183-2186.

Dereje. (2010). *Impact Of Land Use Change On Reservoir*. Addis Abeba: AAU.

Garedew. (2010). *Land-Use and Land-Cover dynamics and rural livelihood perspectives, in the semiarid areas of the central Rift Valley of Ethiopia, PhD thesis, Swedish University of Agricultural Sciences.* Swedish University of Agricultural Sciences.: PhD thesis.

Garg V, Prasun SPA, Bhaskar KG (2017). Assessment of land use land cover change impact on hydrological regime of a basin. Environ Earth Sci 76(18):1–17. https ://doi.org/10.1007/s12665-017-6976-z

Gebrehiwet, K. (2004). Land use land cover changes in centeral highlands of Ethiopia: The case of Yerer mountains and its surroundings. M.Sc Thesis, Addis Ababa University, Environmental Science.

Geremew. (2013). *Assessing the impacts of land use and land cover change on hydrology of watershed: a case study on Gigel-Abbay Watershed, Lake Tana Basin, Ethiopia.* A.A.

Getahun and Van Lanen. (2015). Assessing the Impacts of Land Use-Cover Change on Hydrology of Melka Kuntrie Subbasin in Ethiopia, Using a Conceptual Hydrological Model. *Journal of Waste Water Treatment & Analysis*.

Gwate O, Woyessa Yali E, David Wiberg (2015). International Journal of Environmental Protection and Policy. 3, 31-38.

Hadgu. (2008). Temporal and Spatial changes in land use patterns and biodiversity inrelation to farm productivity at multiple scales in Tigray, Ethiopia. PhD Thesis Wageningen University, Wageningen, The Netherlands.

Gong, Zhe & Kawamura, Kensuke & Ishikawa, N. & Goto, M & Wulan, T & Alateng, D & Yin, T & Ito, Y.. (2015). MODIS normalized difference vegetation index (NDVI) and vegetation phenology dynamics in the Inner Mongolia grassland. Solid Earth. 6. 1185-1194. 10.5194/se-6-1185-2015

Gonfa, Z.B., & Kumar, D. (2016). Application of Soil and Water Assessment Tool Model to Estimate Runoff and Sediment Yield from Mojo Watershed. International Journal of Innovative Research in Science, Engineering and Technology Vol. 5, Issue 2, February 2016

Herold. (2003). The spatiotemporal form of urban growth: Measurement, analysis and modeling. Remote Sens. Environ. *6*, 286.

Horowitz, A. J. (2003). An evaluation of sediment rating curves for estimating suspended sediment concentrations for subsequent flux calculations. *Hydrological Processes,, 17*, 3387–3409.

Ismail, M., Pakhriazad, H., and Shahrin, M. (2009). Evaluating supervised and unsupervised techniques for land cover mapping using remote sensing data. Malaysia Journal of Society and space 5(1), 1–10.

Jensen, J. (2004). Introductory digital image processing: a remote sensing perspective (2nd ed., p. 544). New Jersey: Prentice-Hall.

Juang J, Porporato A, Stoy PC, Siqueira MS, Oishi AC, Detto M et al (2007) Hydrologic and atmospheric controls on initiation of convective precipitation events. Water Resour Res 43:1–10. https :// doi.org/10.1029/2006W R0049 54

Julien. (2010). Erosion and Sedimentation. *2nd ed. xviii + 371 pp. Cambridge University Press. Geological Magazine.*, 683-684.

Kassa. (2009). Watershed Hydrological Responses to Changes in Land Use and Land Cover, and Management Practices at Hare Watershed, Ethiopia.

Kashaigili and Majaliwa, A. M. Implications of land use and land cover changes on hydrological regimes of the Malagarasi River, Tanzania Journal of agricultural sciences and applications, 2013; 2(1): 45-50

Kaushal SS, Gold AJ, Mayer PM (2017) Land use, climate, and water resources-global stages of interaction. Water. https ://doi.org/10.3390/w9100 815

L. Mango et al., A. M. (2011). Land use and climate change impacts on the hydrology of the upper. *Hydrol. Earth Syst*, 2245–2258.

Lambin. (2003). Dynamics of Land-use and land-cover change in tropical regions. Annu. Rev. Environ. Resour. 20. 49205-41. *Annu. Rev. Environ. Resource, 20*, 205-246.

Lilleesand, T. M., Kiefer, R. W., and Chipman, J. W. (2004). Remote sensing and image interpretation (5th ed., p. 763). New York: John Wiley and Sons, Inc.

Masek. (2009). Dynamics of urban growth in the Washington DC metropolitan area,. *International Journal of Remote Sensing, 21*, 3473-3486.

Minta et al., M. K. (2017, September). Land use and land cover dynamics in Dendi-Jeldu hilly-mountainous areas in the central Ethiopian highlands. Geoderma. *elsevier, 314*, 27-36.

Mukete et al., B. &. (2018). Assessing the drivers of land use change in the Rumpi hills forest protected area, Cameroon. *Journal of Sustainable Forestry, 10*, 1-27.

Neitsch et al., A. J. (2011). Soil and water assessment tool users manual version 2000.Rep GSWRL Report 02-02, BRC Report 02-06. Texas Water Resources Institute TR-192., Collage Station,TX.

Qian et al., Q. J. (2007). Comparison of pixel-based and object-oriented classification methods for extracting built-up areas in arid zone. *In: ISPRS Workshop on Updating Geo-Spatial Databases with Imagery & the 5th ISPRS Workshop on DMGISs,*.

Raes, D., Mallants, D., & Song, Z. (1996). Rainbow Software Package for Analyzing Hydrologic Data. Transactions on Ecology and the Environment. ISSN Vol 12., 17433541.

Rogan. (2004). Remote sensing technology for mapping and monitoring land-cover and land-use change. Progress in Planning. 2004;61(4):301-25.2004;61(4):301-25.

Shewangizaw, D., and Michael, Y. (2010). Assessing the effect of land use change on the hydraulic regime of Lake Awassa. Nile Basin Water Science and Engineering, 3(2), 110–118.

Shooshtari SJ, Shayesteh K, Gholamalifard M, Azari M, Notivoli RS, Moreno JIL (2017) Impacts of futureland cover and climate change on the water balance in northern Iran. Hydrol Sci J 62(16):2655–2673. https ://doi.org/10.1080/02626 667.2017.14030 28

Stolbovoi. (2002). Monitoring urban land cover change: An expert system approach to land cover classification of semiarid to arid urban centers.

SWRRB. (n.d.). Simulator for Water Resources in Rural Basins.

Tesfa and Gebremariam. (2016). Impact-Of-Land-Use-Land-Cover-Change-On-Stream-Flow-And-Sediment-Yield-A-Case-Study-Of-Gilgel-Abay-Watershed-Lake-Tana-

Sub-basin-Ethiopia. *International Journal of Technology Enhancements and Emerging Engineering Research*, 28-42.

Tessema, S. &. (2015). Watershed Modeling as a Tool for Sustainable Water Resources Management: SWAT Model Application in the Awash River Basin, Ethiopia. 10.1007/978-3-319-12194-9_30.

Toxopeus W. Ouyang, F. Hao, A.K. Skidmore, A.G. (2010). Soil erosion and sediment yield and their relationships with vegetation cover in upper stream of the Yellow River. *Science of the Total Environment, 409*, 396-403.

Tripathi et al., M. P. (2005). Development of effective management plan for critical subwatersheds using SWAT model. Hydrological Processes. *19*, 809-826.

Tufa. (2015). Impact of water Abstraction on the water level of Lake Ziway, Ethiopia. *Water and Society, V67*, 68-80.

Upadhya and Pandey, U. S. (2012). Annual sedimentation yield and sediment characteristics of upper lake. *journal of chemical science*, 65–74.

US-ACE. (2011). Hydrologic Modeling System HEC- HMS. User's.

Wagner PD, Kumar S, Schneider K (2013). An assessment of land use change impacts on the water resources of the Mula and Mutha Rivers catchment upstream of Pune, India. . *Hydrol Earth Syst Sci Discuss. https ://doi.org/10.5194/hess-17-2233-2013*

Wei, O., Hao, F.H., Skidmor, A.K., Toxopeus, A.G., 2010. Soil erosion and sediment yield and their relationships with vegetation cover in upper stream of the Yellow River. Science of the Total Environment , 409, 396-403.

Willems. (2000). Probabilistic Immission Modelling of Receiving Surface Waters. *Ph.D. Thesis*.

Williams, J. (1997). Sediment routing for agricultural watersheds. Water Resources. *11(5)*, 965-974.

Yao et al., J. T. (2014). Appling SWAT model to explore the impact of changes in land use and climate on the streamflow in a watershed of Northern China. *Shengtai Xuebao/ Acta Ecologica Sinica, 34*.

Zhang et al., J. L. (2014). “Spatiotemporal characteristics, patterns, and causes of land-use changes in China since the late 1980s,”. *Journal of Geographical Sciences, vol. 24, no. 2, pp. 195–210, 2014., 24*, 195-210.

APPENDICES

Appendix Table 1: Performance rating table (Moriasi et al., 2007)

Performance rating	**RSR**	**NSE**	**PBIAS for Stream flow**	**PBIAS for sediment yield**
Very good	0.0≤RSR≤0.5	0.75≤NSCE≤1	PBIAS≤±10	PBIAS<±15
Good	0.5≤RSR≤0.6	0.65<NSCE<0.75	±10≤PBIAS≤15	±15≤PBIAS≤±30
Satisfactory	0.6≤RSR≤0.7	0.5<NSCE<0.65	±15≤PBIAS≤25	±30≤PBIAS≤±55
Unsatisfactory	RSR>0.5	NSCE<0.5	PBIAS≥±25	PBIAS≥±55

Appendix Table 2: Error matrix for classification of 1989

Class Name	**Reference Totals**	**Classified Totals**	**Number Correct**	**Producer Accuracy**	**User Accuracy**
Bare Land	25	22	20	80.00%	90.91%
Water Body	7	10	7	100.00%	70.00%
Built-up	25	25	21	84.00%	84.00%
Forest Land	15	17	13	86.67%	76.47%
Shrub Land	21	20	17	80.95%	85.00%
Agricultural Land	87	86	79	90.80%	91.86%
Totals	180	180	157		
Over all accuracy= 87.22%					
Over all Kappa statistics=0.82					

Appendix Table 3: Error matrix for classification of 1999

Class Name	Reference Totals	Classified Totals	Number Correct	Producer Accuracy	User Accuracy
Built-up	23	25	21	91.30%	84.00%
Water Body	10	10	10	100.00%	100.00%
Bare Land	27	26	25	92.59%	96.00%
Shrub Land	45	55	45	100.00%	81.82%
Forest	14	16	14	100.00%	87.50%
Agricultural Land	61	48	48	78.69%	100.00%
Totals	180	180	163		
Over all accuracy= 90.56%					
Over all Kappa statistics=0.88					

Appendix Table 4: Error matrix for the classification of 2009

Class Name	Reference Totals	Classified Totals	Number Correct	Producer Accuracy	User Accuracy
Built-up	23	25	22	95.65%	88.00%
Water Body	10	10	10	100.00%	100.00%
Bare Land	27	26	25	92.59%	96.15%
Shrub Land	45	55	45	100.00%	81.82%
Forest	15	16	15	100.00%	93.75%
Agricultural Land	60	48	48	80.00%	100.00%
Total	180	180	165		
Over all accuracy= 91.67%					
Over all Kappa statistics=0.89					

Appendix Table 5: Error matrix for the classification of 2018

Class Name	Reference Totals	Classified Totals	Number Correct	Producer Accuracy	User Accuracy
Water Body	6	10	6	100.00%	60.00%
Bare Land	21	24	19	90.48%	79.17%
Shrub Land	26	24	21	80.77%	87.50%
Forest	11	12	11	100.00%	91.67%
Built-up	24	21	20	83.33%	95.24%
Agricultural Land	91	89	84	92.31%	100.00%
Total	179	180	161		
Over all accuracy= 89.44%					
Over all Kappa statistics=0.84					

Appendix Table 6: Annual rainfall data for four meteorological stations

Year	Modjo	Chefe Donsa	Debrezeyit	Ejere
1989	2.831780822	3.047790055	1.849589041	1.900822
1990	2.571232877	2.630494505	2.481593407	2.635068
1991	2.407123288	2.519726027	3.256438356	1.998356
1992	2.180327869	2.318237705	2.426775956	0.201913
1993	2.272876712	2.674657534	3.386849315	2.412603
1994	2.05890411	0.917636986	1.876373626	1.850137
1995	1.841369863	2.000547945	1.617630854	2.08137
1996	4.61010929	1.146106557	2.943715847	2.82377
1997	2.083013699	1.905110034	2.340821918	0.893699
1998	2.83260274	2.49109589	2.697808219	2.907671
1999	0.626849315	1.880906593	2.522739726	2.522466
2000	2.328142077	1.661338798	2.284109589	2.111749
2001	2.159178082	3.517945205	2.368493151	2.523562
2002	1.546027397	1.701917808	1.881917808	2.030137
2003	2.904383562	2.625205479	2.984383562	3.203014
2004	3.530327869	2.178688525	2.329234973	2.600546
2005	3.342191781	2.765342466	2.507671233	2.76
2006	2.835616438	2.551506849	2.737534247	2.856438
2007	3.25890411	2.975616438	2.380821918	2.932055
2008	3.306557377	2.486338798	2.243169399	2.782514
2009	1.650136986	2.331917808	1.753424658	2.140548
2010	3.042191781	3.015342466	2.518082192	2.558082
2011	2.240821918	2.19260274	2.750410959	3.254247
2012	4.397540984	2.475956284	1.876923077	2.540984
2013	3.003835616	3.350136986	2.833424658	2.653699
2014	2.397534247	2.357260274	6.456986301	6.456986
2015	2.354520548	1.880547945	2.7	2.7
2016	4.159562842	2.19726776	4.413661202	4.364481
2017	2.933424658	2.329726027	2.872054795	2.92137
2018	3.091849315	3.315728022	2.927054795	2.923356

Appendix Table 7: Average Annual rainfall patterns of stations

YEAR	Chefe Donsa	Debrezeyit	Modjo	Ejere	Average
1989	1103.30	675.1	28.6564	693.8	625.21
1990	957.50	903.3	32.6691	961.8	713.82
1991	919.70	1188.6	27.9219	729.4	716.41
1992	848.48	888.2	23.0071	73.9	458.40
1993	976.25	1236.2	30.8183	880.6	780.97
1994	334.94	683	19.4159	675.3	428.16
1995	730.20	587.2	22.6296	759.7	524.93
1996	419.48	1077.4	34.2888	1033.5	641.17
1997	693.46	854.4	22.2381	326.2	474.07
1998	909.25	984.7	34.7183	1061.3	747.49
1999	684.65	920.8	26.3225	920.7	638.12
2000	608.05	864.5	24.7336	772.9	567.55
2001	1284.05	864.5	30.7221	921.1	775.09
2002	621.20	686.9	23.2441	741	518.09
2003	958.20	1089.3	33.965	1169.1	812.64
2004	797.40	852.5	30.4213	951.8	658.03
2005	1009.35	915.3	34.725	1007.4	741.69
2006	931.30	999.2	32.6919	1040.9	751.02
2007	1086.10	869	33.837	1070.2	764.78
2008	910.00	821	32.0533	1018.4	695.36
2009	851.15	640	32.2852	781.3	576.18
2010	1100.60	919.1	33.3699	933.7	746.69
2011	800.30	1003.9	31.7907	1187.8	755.95
2012	906.20	683.2	34.3483	930	638.44
2013	1222.80	1034.2	36.6683	968.6	815.57
2014	860.40	2356.8	49.5067	2356.8	1405.88
2015	686.40	985.5	32.7546	985.5	672.54
2016	804.20	1615.4	42.6717	1597.4	1014.92
2017	850.35	1048.3	33.1277	1066.3	749.52
2018	1206.93	1068.375	36.6179	1067.03	844.74
Total	869.07	977.1958	942.22	956.114	931.15

AVE MONTHLY BASIN VALUES

MON	RAIN (MM)	SNOW FALL (MM)	SURF Q (MM)	LAT Q (MM)	WATER YIELD (MM)	ET (MM)	SED YIELD (T/HA)	PET (MM)
1	18.76	0.00	5.54	0.21	10.37	17.75	1.98	57.85
2	33.68	0.00	11.28	0.29	14.94	55.53	2.51	76.67
3	50.93	0.00	11.05	0.46	15.27	61.10	1.72	122.94
4	55.61	0.00	10.11	0.56	13.45	45.15	1.49	105.04
5	57.42	0.00	10.92	0.68	13.36	36.24	1.50	95.45
6	102.76	0.00	22.02	1.01	24.66	38.61	2.86	81.48
7	227.41	0.00	74.38	2.91	82.23	64.85	10.46	92.83
8	226.66	0.00	86.73	4.25	119.57	19.52	12.03	22.72
9	102.97	0.00	32.44	2.56	91.95	39.63	1.51	64.31
10	27.78	0.00	7.97	0.84	56.73	28.98	1.91	93.01
11	14.72	0.00	3.14	0.35	29.23	17.17	0.72	81.78
12	12.93	0.00	3.81	0.24	15.98	2.22	1.22	8.33

Appendix Figure 1: Average monthly values for water balance components of Modjo watershed

	Area [ha]	Area[acres]
Watershed	170256.4197	420736.8357
Number of Subbasins: 29		

	Area [ha]	Area[acres]	%Mat.Area
LANDUSE:			
Water --> WATR	21498.7257	53124.4260	12.63
Range-Grasses --> RNGE	1552.3692	3835.9820	0.91
Forest-Evergreen --> FRSE	23271.0907	57504.0287	13.67
Agricultural Land Generic --> AGRL	61737.8781	152557.3837	36.26
Barren --> BARR	9204.6786	22745.2210	5.41
Residential --> URBN	53001.6769	130969.7937	31.13
SOILS:			
Be9-3c-26	43051.9635	106383.5545	25.29
Ne10-3b-154	3400.9695	8403.9656	2.00
Ne13-3b-158	17031.3861	42085.4067	10.00
Vp14-3a-286	103793.7580	256479.8774	60.96
Xh16-a-309	2988.5413	7384.8350	1.76
SLOPE:			
0-5	154158.2573	380932.7617	90.54
10-15	2938.2302	7260.5138	1.73
15-20	1108.7913	2739.8786	0.65
20-9999	609.7690	1506.7812	0.36
5-10	11451.7715	28297.8999	6.73

Appendix Figure 2: HRU Analysis Report for Land use, Soil and Slope

	Parameter Name	t-Stat	P-Value
▸	11:R__ESCO.hru	-0.004960125	0.996117718
	3:V__GW_DELAY.gw	-0.074202452	0.941978933
	6:R__CH_K2.rte	0.166488965	0.870333773
	12:R__EPCO.hru	-0.218781406	0.830217630
	9:R__SLSUBBSN.hru	-0.259608888	0.799231403
	5:R__CH_N2.rte	0.336301999	0.742009647
	7:R__SOL_AWC(..).sol	0.354158995	0.728898060
	15:R__GW_REVAP.gw	-0.429434163	0.674638970
	16:R__USLE_K(..).sol	-0.557507719	0.586652603
	14:R__SURLAG.bsn	0.558287626	0.586135341
	2:V__ALPHA_BF.gw	-0.578909488	0.572544724
	4:V__GWQMN.gw	0.932463239	0.368092617
	13:R__SOL_ALB(..).sol	0.985377095	0.342424107
	10:R__CANMX.hru	-1.344468686	0.201787748
	8:R__SOL_K(..).sol	1.596147551	0.134468441
	1:R__CN2.mgt	8.139209040	0.000001850

Appendix Figure 3: Global sensitivity analysis values for streamflow

	Parameter Name	t-Stat	P-Value
▸	8:R__LAT_SED.hru	-0.121645753	0.904080427
	7:R__CH_COV2.rte	-0.589614292	0.560351328
	9:R__SPEXP.bsn	-0.609532830	0.547266928
	2:R__CN2.mgt	-0.914284017	0.368660751
	1:R__USLE_K(..).sol	-0.932051399	0.359570122
	10:R__EROS_EXPO.bsn	-1.045041272	0.305270316
	4:R__ADJ_PKR.bsn	-1.307851181	0.201950337
	3:R__SPCON.bsn	-1.430753499	0.163973579
	6:R__USLE_P.mgt	-1.555860990	0.131386269
	5:R__CH_EQN.rte	1.753273955	0.090903231
	12:R__CH_ERODMO(..).rte	-2.928806243	0.006836250
	11:R__BIOMIX.mgt	-5.645540382	0.000005410

Appendix Figure 4: Global sensitivity analysis values for sediment yield